NACA TN 2301

NATIONAL ADVISORY COMMITTEE FOR AERONAUTICS

TECHNICAL NOTE 2301

LINEARIZED SOLUTION AND GENERAL PLASTIC BEHAVIOR OF THIN PLATE WITH CIRCULAR HOLE IN STRAIN-HARDENING RANGE

By M. H. Lee Wu

Lewis Flight Propulsion Laboratory
Cleveland, Ohio

Washington
March 1951

NATIONAL ADVISORY COMMITTEE FOR AERONAUTICS

TECHNICAL NOTE 2301

LINEARIZED SOLUTION AND GENERAL PLASTIC BEHAVIOR OF THIN PLATE WITH CIRCULAR HOLE IN STRAIN-HARDENING RANGE

By M. H. Lee Wu

SUMMARY

A linearized solution is obtained for the problem of plastic deformation of a thin plate with a circular hole in the strain-hardening range. This solution is based on the deformation theory of plasticity for finite strains. The two final simultaneous nonlinear differential equations obtained previously are linearized by replacing the nonlinear terms with a simple linear term involving a constant, which is determined by minimizing the effect due to the linearization. Stress and strain distributions of the problem for a given material and a given maximum strain can be obtained through a simple multiplication by means of the tables presented herein. Equations for stress and strain concentration factor are also given.

Numerical examples are calculated by the linearized method. Calculations are also made for ideally plastic materials and for a power-law approximation. An approximate method of solution for stress is also presented herein. The results obtained by different methods are compared and the following conclusions were obtained:

1. The results obtained by the linearized method compare closely with those obtained previously without linearization.

2. The variation of a parameter determined from the octahedral shear stress-strain curve of the material can be used as a simple general criterion of applicability of deformation theory for this problem.

3. The ratios of the strains along the radius to their maximum values and the ratio of principal stresses are essentially independent of the octahedral shear stress-strain curve of the material, but the stress distributions are very dependent on the material.

4. The solution for ideally plastic material with the infinitesimal strain concept gives good approximate values of strains, but not of stresses.

5. Sufficiently accurate values of principal stresses can be obtained by using the strains determined by the ideally plastic approximation together with the actual octahedral shear stress-strain relation of a given material.

6. If a simple analytical function representing the octahedral shear stress-strain relation is required for analysis, the power-law approximation can be used.

INTRODUCTION

In the design of highly stressed machine parts, knowledge of the stress and strain concentration due to a hole and also of the distributions of stresses and strains in the strain-hardening range is desirable. The solution for a thin plate with a circular hole for ideally plastic material under infinitesimal strain has been obtained by Nádai (reference 1, page 189). The same problem has been solved (reference 2) in the strain-hardening range by using the deformation theory of plasticity and employing the finite-strain concept; numerical results were obtained for two materials in reference 2. Because of the nonlinearity of the equations, however, the results were more or less limited to the two particular materials used in the calculation. In order to obtain general information applicable to most materials, it is desirable to investigate the possibility of linearizing the equations. A linearized solution will also greatly reduce the amount of calculation required for a given case.

Generalization of these results also has theoretical significance in the theory of plasticity in that a general criterion of the applicability of the deformation theory may be obtained. This theory, formulated by Hencky and Nádai (reference 3), states that the state of stress is a unique function of the state of strain when the directions and the ratios of the principal stresses remain constant during loading in the absence of time and temperature effects and of unloading. It is true for plastic deformations, which are irreversible processes, that the plastic strains at a certain state depend on the path by which that state is reached. For a particular path, the relations between the state of strain and stress are unique if the material is isotropic before loading, as is generally assumed. Experiments on thin tubes (references 4 to 10) show that the relations between the strain and the stress for the different

paths, each under a constant ratio of principal stresses (also constant directions), are close. The results obtained by the deformation theory therefore have physical significance if the previously mentioned conditions (the directions and the ratios of principal stresses remain constant during loading) are satisfied. No inconsistency exists in the deformation theory if it is used for the cases where these conditions are fulfilled. Even with considerable variation of the ratios and directions of principal stresses during loading, the strains experimentally obtained were in good agreement with the strains predicted by use of the deformation theory, as shown in references 9 (p. 199), 10 (pp. 213-15), and 11, and also in experimental work presented by the NACA at the Third Symposium on Plasticity at Brown University. Further experimental investigation is needed to determine the extent to which the variations of directions and ratios of principal stresses are permissible. If the variation is small, however, the deformation theory can be expected to give good results.

The simplicity of the stress-strain relation given by the deformation theory minimizes the difficulties of solving concrete problems; it is therefore of both theoretical and practical importance to investigate the circumstances (stress-strain curves of materials, loading conditions, boundary conditions, and geometry of the members) under which the deformation theory applies.

SYMBOLS

The following symbols are used in this report:

A,B,C, D,E,F	coefficients of nonlinear differential equations; functions of α and γ
a	inner radius of hole
b	outer radius of flat ring
c	outer radius of plate, very large compared with radius a
H,J,L	functions of α
h	instantaneous thickness of plate
h_{init}	initial thickness of plate
l	instantaneous length

m parameter relating to strain hardening

n parameter relating to criterion of applicability of deformation theory

r radial coordinate

u radial displacement

α parameter indicating ratio of principal stresses

γ octahedral shear strain

ϵ logarithmic strain (or natural strain), logarithm of instantaneous length divided by initial length of element

θ angular coordinate

σ normal true stress, force per unit instantaneous area

τ octahedral shear stress

Subscripts:

o at inner radius of hole

b,c at radii b and c, respectively

j principal direction in general

r,θ,z principal directions in cylindrical coordinate system

BASIC EQUATIONS

A thin infinite plate uniformly stressed in its plane in all directions and having a circular hole is shown in figure 1. The whole system is equivalent to a very large circular plate of radius c with a small concentric circular hole subjected radially to the same uniform stresses σ on the outer boundary. The solution obtained in such a plate within any radius b can be also considered as a solution of a flat ring with inner radius a and outer radius b loaded uniformly at the outer boundary with the radial stress σ_b obtained in the plate solution. A small element defined by $\Delta\theta$ and $\Delta(r+u)$ taken at radius $(r+u)$ in the deformed state is also shown in figure 1. In the undeformed state, the same

element would be at radius r and defined by $\Delta\theta$ and Δr. Also shown in figure 1 are the instantaneous thickness of the element and the stresses acting on the element.

The stress and strain relations based on the deformation theory for the case of plane plastic stress are

$$\epsilon_\theta + \epsilon_r + \epsilon_z = 0 \tag{1}$$

$$\tau = \frac{\sqrt{2}}{3}\left(\sigma_r^2 - \sigma_r \sigma_\theta + \sigma_\theta^2\right)^{\frac{1}{2}} \tag{2a}$$

$$\gamma = 2\sqrt{\frac{2}{3}}\left(\epsilon_r^2 + \epsilon_r \epsilon_\theta + \epsilon_\theta^2\right)^{\frac{1}{2}} \tag{2b}$$

$$\tau = \tau(\gamma) \tag{3}$$

$$\epsilon_\theta = \frac{1}{3}\frac{\gamma}{\tau}\left(\sigma_\theta - \frac{1}{2}\sigma_r\right) \tag{4a}$$

$$\epsilon_r = \frac{1}{3}\frac{\gamma}{\tau}\left(\sigma_r - \frac{1}{2}\sigma_\theta\right) \tag{4b}$$

$$\epsilon_z = \frac{1}{3}\frac{\gamma}{\tau}\left[-\frac{1}{2}\left(\sigma_\theta + \sigma_r\right)\right] \tag{4c}$$

where $\tau(\gamma)$ is an experimentally determined function. The constants 1/2 and 1/3 in equations (4) are determined from the condition defined by equation (1) and one of the equation (2). Only five of these given equations are therefore independent.

The finite-strain concept (references 3 and 12), which considers the instantaneous dimensions of the element, is used because large deformations in the strain-hardening range will be considered. The stress is then equal to the force divided by the instantaneous area, and the strains are defined by the following equations:

$$\Delta\epsilon_j = \frac{\Delta l_j}{l_j}$$

where l_j is the instantaneous length of an element having the original length of $(l_j)_o$ and j is any principal direction. The octahedral shear stress-strain relation, the value of octahedral shear strain, and the value of the principal strains are defined by the initial and final states for the paths along which the ratios of principal stresses remain constant during loading (reference 2); thus,

$$\epsilon_j = \log_e \frac{l_j}{(l_j)_o} \quad \text{or} \quad e^{\epsilon_j} = \frac{l_j}{(l_j)_o}$$

The strain given by this equation has been referred to as "logarithmic strain or natural strain" (references 3 and 12). The strain-displacement relations of the element shown in figure 1 are

$$e^{\epsilon_r} = \frac{d(r+u)}{dr} \tag{5a}$$

$$e^{\epsilon_\theta} = \frac{r+u}{r} \tag{5b}$$

$$e^{\epsilon_z} = \frac{h}{h_{init}} \tag{5c}$$

The equations of equilibrium and compatibility after the elimination of the displacements and ϵ_z (obtained in reference 2) are as follows:

$$\left(\frac{r}{a}\right)\frac{d\sigma_r}{d\left(\frac{r}{a}\right)} - \sigma_r\left(\frac{r}{a}\right)\frac{d(\epsilon_r + \epsilon_\theta)}{d\left(\frac{r}{a}\right)} = (\sigma_\theta - \sigma_r)\, e^{\epsilon_r - \epsilon_\theta} \tag{6a}$$

$$\left(\frac{r}{a}\right)\frac{d\epsilon_\theta}{d\left(\frac{r}{a}\right)} = e^{\epsilon_r - \epsilon_\theta} - 1 \tag{6b}$$

Equations (2b), (3), (4a) (4b), (6a), and (6b) are six equations with six unknowns, σ_r, σ_θ, ϵ_r, ϵ_θ, τ, and γ. By using the transformations of references 1 (p. 189), 2, and 13,

$$\sigma_\theta + \sigma_r = 3\sqrt{2}\,\tau \sin\alpha$$

$$\sigma_\theta - \sigma_r = \sqrt{6}\,\tau\cos\alpha$$

or

$$\left.\begin{aligned}\sigma_r &= \sqrt{\frac{3}{2}}\,\tau\left(\sqrt{3}\sin\alpha - \cos\alpha\right)\\ \sigma_\theta &= \sqrt{\frac{3}{2}}\,\tau\left(\sqrt{3}\sin\alpha + \cos\alpha\right)\end{aligned}\right\} \tag{7}$$

and

$$\left.\begin{aligned}\epsilon_r &= \frac{\gamma}{2\sqrt{2}}\left(\sin\alpha - \sqrt{3}\cos\alpha\right)\\ \epsilon_\theta &= \frac{\gamma}{2\sqrt{2}}\left(\sin\alpha + \sqrt{3}\cos\alpha\right)\end{aligned}\right\} \tag{8}$$

The parameter α is closely related to the ratio of principal stresses σ_r/σ_θ. From equation (7),

$$\frac{\sigma_r}{\sigma_\theta} = \frac{\sqrt{3}\sin\alpha - \cos\alpha}{\sqrt{3}\sin\alpha + \cos\alpha}$$

This relation is plotted in figure 2 for the range of α encountered in the present problem. It is seen that σ_r/σ_θ varies almost linearily with α. The percentage variation of α during loading will then indicate directly the same percentage variation of σ_r/σ_θ. When this transformation is used, the equations of the problem are then reduced to two nonlinear differential equations with an experimentally determined relation between τ and γ.

$$\left.\begin{aligned}A\left(\frac{r}{a}\right)\frac{d\alpha}{d\left(\frac{r}{a}\right)} + B\left(\frac{r}{a}\right)\frac{d\gamma}{d\left(\frac{r}{a}\right)} &= C\\ D\left(\frac{r}{a}\right)\frac{d\alpha}{d\left(\frac{r}{a}\right)} + E\left(\frac{r}{a}\right)\frac{d\gamma}{d\left(\frac{r}{a}\right)} &= F\end{aligned}\right\} \tag{9}$$

where

$$\left.\begin{aligned}
A &= \left[\left(\sqrt{3}\cos\alpha + \sin\alpha\right) - \left(\sqrt{3}\sin\alpha - \cos\alpha\right)\frac{\gamma\cos\alpha}{\sqrt{2}}\right] \\
B &= \left(\sqrt{3}\sin\alpha - \cos\alpha\right)\left(\frac{\gamma}{\tau}\frac{d\tau}{d\gamma} - \frac{\gamma\sin\alpha}{\sqrt{2}}\right)\frac{1}{\gamma} \\
C &= 2(\cos\alpha)\exp\left(-\sqrt{\frac{3}{2}}\gamma\cos\alpha\right) \\
D &= \left(\sqrt{3}\sin\alpha - \cos\alpha\right)\gamma \\
E &= -\left(\sqrt{3}\cos\alpha + \sin\alpha\right) \\
F &= 2\sqrt{2}\left[1 - \exp\left(-\sqrt{\frac{3}{2}}\gamma\cos\alpha\right)\right]
\end{aligned}\right\} \quad (9a)$$

From equations (9), there is obtained

$$\left.\begin{aligned}
\left(\frac{r}{a}\right)\frac{d\alpha}{d\left(\frac{r}{a}\right)} &= \frac{CE - FB}{AE - DB} \\
\left(\frac{r}{a}\right)\frac{d\gamma}{d\left(\frac{r}{a}\right)} &= \frac{FA - CD}{EA - BD}
\end{aligned}\right\}$$

If α is considered as an independent variable, the calculation can be greatly reduced because many terms in the equations are trigonometric functions of α; that is,

$$\left.\begin{aligned}
\frac{d\log_e\left(\frac{r}{a}\right)}{d\alpha} &= \frac{AE - DB}{CE - BF} \\
\frac{d\gamma}{d\alpha} &= \frac{FA - CD}{CE - FB}
\end{aligned}\right\} \quad (10)$$

Using equations (9a) and expanding $\exp\left(-\sqrt{\frac{3}{2}}\gamma\cos\alpha\right)$ into a series gives

$$\left.\begin{aligned} CE - BF &= -2HL - 2\sqrt{3}\,HJ\; g\left(\alpha,\gamma,\frac{\gamma}{\tau}\frac{d\tau}{d\gamma}\right) f_1(\alpha,\gamma) \\ AF - CD &= \left\{8H^2 - 2\sqrt{3}\,HL\left[1 - f_1(\alpha,\gamma)\right]\right\}\gamma \\ AE - BD &= -L^2 - J^2\; g\left(\alpha,\gamma,\frac{\gamma}{\tau}\frac{d\tau}{d\gamma}\right) \end{aligned}\right\} \qquad (10a)$$

where

$$H = \cos\alpha$$

$$J = \sqrt{3}\sin\alpha - \cos\alpha$$

$$L = \sqrt{3}\cos\alpha + \sin\alpha$$

and

$$f_1(\alpha,\gamma) = \frac{1}{\sqrt{\frac{3}{2}}(\cos\alpha)\gamma}\left[1 - e^{-\sqrt{\frac{3}{2}}(\cos\alpha)\gamma}\right]$$

$$= 1 - \frac{1}{2}\sqrt{\frac{3}{2}}(\cos\alpha)\gamma + \frac{1}{4}(\cos^2\alpha)\gamma^2 \ldots$$

$$g\left(\alpha,\gamma,\frac{\gamma}{\tau}\frac{d\tau}{d\gamma}\right) = \frac{\gamma}{\tau}\frac{d\tau}{d\gamma} - \sqrt{\frac{3}{2}}\frac{1}{J}\gamma$$

LINEARIZATION OF EQUATIONS

Substituting equations (10a) into equations (10) yields the following equations:

$$\frac{d\,\log_e\left(\frac{r}{a}\right)}{d\alpha} = \left(\frac{L}{2H}\right)\frac{1 + \left(\frac{J}{L}\right)^2\left[\frac{\gamma}{\tau}\frac{d\tau}{d\gamma} - \left(\sqrt{\frac{3}{2}}\frac{1}{J}\frac{\gamma}{\gamma_o}\right)\gamma_o\right]}{1 + \sqrt{3}\left(\frac{J}{L}\right)\left[\frac{\gamma}{\tau}\frac{d\tau}{d\gamma} - \left(\sqrt{\frac{3}{2}}\frac{1}{J}\frac{\gamma}{\gamma_o}\right)\gamma_o\right]\left(1 - \frac{1}{2}\sqrt{\frac{3}{2}}H\gamma + \frac{1}{4}H^2\gamma^2 - \ldots\right)} \qquad (11a)$$

$$\frac{d \log_e \gamma}{d\alpha} = \left(-\frac{4H}{L}\right) \frac{1 - \frac{3}{8\sqrt{2}} L\gamma + \frac{\sqrt{3}}{16} LH\gamma^2 - \cdots}{1 + \sqrt{3}\left(\frac{J}{L}\right)\left[\frac{\gamma}{\tau}\frac{d\tau}{d\gamma} - \left(\sqrt{\frac{3}{2}}\frac{1}{J}\frac{\gamma}{\gamma_o}\right)\gamma_o\right]\left(1 - \frac{1}{2}\sqrt{\frac{3}{2}} H\gamma + \frac{1}{4} H^2\gamma^2 - \cdots\right)} \tag{11b}$$

It is seen in the previous equations that τ always occurs in the combination $\frac{\gamma}{\tau}\frac{d\tau}{d\gamma}$. When a $\tau(\gamma)$ curve of a material is plotted in logarithmic scale, the slope of the curve at any value of γ is

$$\frac{d \log_e \tau}{d \log_e \gamma} = \frac{\gamma}{\tau}\frac{d\tau}{d\gamma}$$

The slope $\frac{\gamma}{\tau}\frac{d\tau}{d\gamma}$ in the logarithmic plotting is a function of γ. The use of the power function relating to the octahedral shear stress and strain, which approximates the actual octahedral shear stress-strain relation of a given material over the strain-hardening range, will be subsequently shown to give results approximately the same as those obtained by using the actual octahedral shear stress-strain curve of the material. The power-function relation (or power-law approximation) can be represented by the following equation:

$$\tau(\gamma) = K\gamma^m$$

or

$$\frac{\gamma}{\tau}\frac{d\tau}{d\gamma} = m \tag{12}$$

where K and m are constants through the strain-hardening range. If equation (12) is used only to represent the τ and γ relation for the range of γ along the radius of the plate, accurate results can be expected. It should be emphasized in such a case that the value of m for one material is different for different loads. When the value of γ_o is decided for any calculation, the range of γ can be estimated because the values γ_o/γ_b are quite close for different cases (reference 2). The value of m is then simply the slope of a straight line that approximates the $\tau(\gamma)$ curve of the actual material plotted in the logarithmic scale for the range γ_b to γ_o. The term $\frac{\gamma}{\tau}\frac{d\tau}{d\gamma}$ in equations (11) can then be replaced by m.

A comparison of the terms in equations (11a) and (11b) with the numerical data obtained in reference 2 shows that $\left(\frac{J}{L}\right)^2\left(\sqrt{\frac{3}{2}}\frac{1}{J}\frac{\gamma}{\gamma_o}\right)\gamma_o$, $\left(-\frac{1}{2}\sqrt{\frac{3}{2}}H\gamma+\frac{1}{4}H^2\gamma^2-\ldots\right)$, $\sqrt{3}\frac{J}{L}\left(\sqrt{\frac{3}{2}}\frac{1}{J}\frac{\gamma}{\gamma_o}\right)\gamma_o$, and $\left(-\frac{3}{8\sqrt{2}}L\gamma+\frac{\sqrt{3}}{16}LH\gamma^2-\ldots\right)$ are small compared with $\left[1+\left(\frac{J}{L}\right)^2\frac{\gamma}{\tau}\frac{d\tau}{d\gamma}\right]$, 1, $\left[1+\sqrt{3}\frac{J}{L}\frac{\gamma}{\tau}\frac{d\tau}{d\gamma}\right]$, and 1, respectively. Equations (11) can therefore be linearized by replacing the term $\sqrt{\frac{3}{2}}\frac{1}{J}\frac{\gamma}{\gamma_o}$ by a constant C_1, which is so determined that the effect on $\frac{d\log_e\left(\frac{r}{a}\right)}{d\alpha}$ due to replacing $\sqrt{\frac{3}{2}}\frac{1}{J}\frac{\gamma}{\gamma_o}$ by C_1 and neglecting the terms $\left(-\frac{1}{2}\sqrt{\frac{3}{2}}H\gamma+\frac{1}{4}H^2\gamma^2-\ldots\right)$ in equation (11a), as well as the effect on $\frac{d\log_e\gamma}{d\alpha}$ due to replacing $\sqrt{\frac{3}{2}}\frac{1}{J}\frac{\gamma}{\gamma_o}$ by C_1 and neglecting the terms $\left(-\frac{3}{8\sqrt{2}}L\gamma+\frac{\sqrt{3}}{16}LH\gamma^2-\ldots\right)$ and $\left(-\frac{1}{2}\sqrt{\frac{3}{2}}H\gamma+\frac{1}{4}H^2\gamma^2-\ldots\right)$ in equation (11b), is very small. Equations (11) are then written in the following form:

$$\frac{d\log_e\left(\frac{r}{a}\right)}{d\alpha}=\left(\frac{L}{2H}\right)\frac{1+\left(\frac{J}{L}\right)^2(m-C_1\gamma_o)}{1+\sqrt{3}\frac{J}{L}(m-C_1\gamma_o)} \tag{13a}$$

$$\frac{d\log_e\gamma}{d\alpha}=\left(-\frac{4H}{L}\right)\frac{1}{1+\sqrt{3}\frac{J}{L}(m-C_1\gamma_o)} \tag{13b}$$

Let

$$n=m-C_1\gamma_o \tag{14}$$

then

$$\frac{d \log_e \left(\frac{r}{a}\right)}{d\alpha} = \left(\frac{J}{2\sqrt{3}H}\right) \frac{\left(\frac{L}{J}\right)^2 + n}{\left(\frac{L}{\sqrt{3}} \frac{1}{J}\right) + n}$$

$$\frac{d \log_e \gamma}{d\alpha} = \left(-\frac{4H}{\sqrt{3}J}\right) \frac{1}{\left(\frac{L}{\sqrt{3}J}\right) + n}$$

or

$$\frac{r}{a} = \exp\left[\int_{\alpha_o}^{\alpha} \left(\frac{J}{2\sqrt{3}H}\right) \frac{\left(\frac{L}{J}\right)^2 + n}{\left(\frac{L}{\sqrt{3}J}\right) + n} d\alpha\right] \tag{15a}$$

$$\frac{\gamma}{\gamma_o} = \exp\left[\int_{\alpha_o}^{\alpha} -\left(\frac{4H}{\sqrt{3}J}\right) \frac{1}{\left(\frac{L}{\sqrt{3}J}\right) + n} d\alpha\right] \tag{15b}$$

In equations (15) all terms under the integral sign are functions of α except n, which is a constant. The values of r/a and γ/γ_o corresponding to α for various values of n can therefore easily be calculated by numerical integration. The constant C_1 in equation (14) can be determined either by comparing the variations of α and γ/γ_o with r/a for different values of n calculated from equations (15) with those obtained in reference 2, or by comparing the terms in equations (11). (Because the relations of the variables α, γ/γ_o, and r/a for different cases obtained in reference 2 are very similar, any available relations of these variables for the problem can be used to compare the terms in equations (11) in determining the constant C_1.) The value of C_1 was found to be 0.7 by the first method. Thus,

$$n = m - 0.7\,\gamma_o \tag{14a}$$

With this method, the values of r/a and γ/γ_o corresponding to α for a number of values of n can easily be calculated and given in both curve and tabular form to facilitate solution of this problem for a given material under a given maximum strain.

DETERMINATION OF PRINCIPAL STRESSES AND STRAINS

After the variation of α and γ/γ_o with r/a is determined by the manner previously described, the principal stresses and strains can be obtained by equations (7) and (8) with the actual $\tau(\gamma)$ curve of a given material. It is seen from the equations that ϵ_r/γ, ϵ_θ/γ, σ_r/τ, and σ_θ/τ are functions of α only; they can be calculated for different values of α and given in tabular form to facilitate solution of any given case. Equations (7) and (8) can be written as

$$\left.\begin{aligned} \sigma_r/\tau &= \sqrt{\frac{3}{2}}\left(\sqrt{3}\sin\alpha - \cos\alpha\right) \\ \sigma_\theta/\tau &= \sqrt{\frac{3}{2}}\left(\sqrt{3}\sin\alpha + \cos\alpha\right) \end{aligned}\right\} \tag{7a}$$

$$\left.\begin{aligned} \epsilon_r/\gamma &= \frac{1}{2\sqrt{2}}\left(\sin\alpha - \sqrt{3}\cos\alpha\right) \\ \epsilon_\theta/\gamma &= \frac{1}{2\sqrt{2}}\left(\sin\alpha + \sqrt{3}\cos\alpha\right) \end{aligned}\right\} \tag{8a}$$

The value of principal stresses and strains can be then obtained only by a simple multiplication.

The method of determining the distribution of α, γ/γ_o, σ_r, σ_θ, ϵ_r, and ϵ_θ along r/a will be designated the linearized solution.

STRESS AND STRAIN CONCENTRATION FACTORS AT HOLE

The stress and strain concentration factors are defined as the ratio of tangential stress and strain at the hole to the tangential

stress and strain at $r = c$, respectively, with c/a much greater than 1. For the previously described loading condition, the values of α at boundaries are as follows:

at $r = a$,

$$\sigma_r = 0$$

$$\alpha_o = \frac{\pi}{6}$$

at $r = c$,

$$\sigma_r = \sigma_\theta$$

$$\alpha_c = \frac{\pi}{2}$$

From equation (7), the stress concentration factor is

$$\frac{(\sigma_\theta)_o}{(\sigma_\theta)_c} = \frac{\tau_o\left(\sqrt{3}\sin\frac{\pi}{6} + \cos\frac{\pi}{6}\right)}{\tau_c\left(\sqrt{3}\sin\frac{\pi}{2} + \cos\frac{\pi}{2}\right)} = \frac{\tau_o}{\tau_c} \tag{16a}$$

From equation (8), the strain concentration factor is

$$\frac{(\epsilon_\theta)_o}{(\epsilon_\theta)_c} = \frac{\gamma_o\left(\sin\frac{\pi}{6} + \sqrt{3}\cos\frac{\pi}{6}\right)}{\gamma_c\left(\sin\frac{\pi}{2} + \sqrt{3}\cos\frac{\pi}{2}\right)} = \frac{2\gamma_o}{\gamma_c} \tag{16b}$$

The stress and strain concentration factors were experimentally determined in reference 14 for a tension panel with a circular hole. An approximate equation of stress concentration factor for the same problem was given in reference 15.

IDEALLY PLASTIC AND APPROXIMATE SOLUTION

When $n = 0$, equations (15) become

$$\frac{r}{a} = \exp\left\{\int_{\alpha_o}^{\alpha}\left[\frac{\sqrt{3}}{2}\,d\alpha - \frac{1}{2}\,d\,(\log_e\cos\alpha)\right]\right\}$$

$$\frac{\gamma}{\gamma_o} = \exp\left(\int_{\alpha_o}^{\alpha} - \frac{4\,d\alpha}{\sqrt{3} + \tan\alpha}\right)$$

$$\left(\frac{r}{a}\right)^2 = \frac{\cos \alpha_o}{\cos \alpha} e^{\sqrt{3}(\alpha - \alpha_o)} \tag{17a}$$

$$\frac{\gamma}{\gamma_o} = \frac{\sqrt{3} \cos \alpha_o + \sin \alpha_o}{\sqrt{3} \cos \alpha + \sin \alpha} e^{\sqrt{3}(\alpha_o - \alpha)} \tag{17b}$$

For ideally plastic material when the infinitesimal strain concept is employed, $m = 0$ and γ_o is infinitesimal; n is then equal to zero, this being the special case of $n = 0$. For this case, the same relation between r/a and α as in equation (17a) was obtained by Nádai (reference 1).

The variation of α and γ/γ_o with r/a for a material with $n \neq 0$ can be determined approximately by equations (17). This approximation, however, is used only to determine strains ϵ_r and ϵ_θ because the strains are functions of α and γ only. The stresses, which are functions of α and τ, can be determined by the approximate values of α and γ/γ_o with the actual $\tau(\gamma)$ curve of the material. This method will be designated the approximate solution.

CALCULATIONS, RESULTS, AND DISCUSSION

In order to observe the degree of approximation resulting from the use of a power function representing the octahedral shear stress-strain relation over the whole strain-hardening range, a calculation is made with the following relation between τ and γ:

$$\tau(\gamma) = 126{,}000\ \gamma^{0.25}$$

The constants 126,000 and 0.25 are chosen in order to approximate the $\tau(\gamma)$ curve of Inconel X over the whole strain-hardening range (fig. 3). The variations of α, γ, σ_r, σ_θ, ϵ_r, and ϵ_θ with r/a for $\gamma_o = 0.3$ obtained by the power-law approximation are compared with the values obtained from the actual $\tau(\gamma)$ curve of Inconel X in figure 4. These curves are seen to agree well. This result indicates that the method used to linearize $\frac{\gamma}{\tau}\frac{d\tau}{d\gamma}$ in equations (11)

should introduce very little error. Also, if a simple analytical function of $\tau(\gamma)$ is desired in the analysis, this simple form $\tau(\gamma) = K\gamma^m$ representing the τ and γ relation of a given material will give a very good approximation.

The values of r/a and γ/γ_o corresponding to α are calculated for $n = -0.15, -0.1, 0, 0.1, 0.2, 0.3$, and 0.4 from the linearized equations (15). The variations of α and γ/γ_o with r/a for different values of n are plotted in figure 5 and are tabulated in table I. The curves of α and γ/γ_o against r/a obtained in reference 2 for Inconel X and 16-25-6 are plotted in figure 6; the values of n for these cases are calculated from equation (14a) and are also indicated on these curves. The curves obtained from the linearized solution (fig. 5), which have values of n close to the values of n of the curves obtained from reference 2, are also plotted on figure 6 for comparison. It can be seen that the results for the same n of the two solutions agree very well for most cases. For simplicity, the solutions obtained in reference 2 based on the deformation theory are designated the exact solution. The simple relation $n = m - 0.7\,\gamma_o$ can then be used as a good approximate criterion to find the distributions of α and γ/γ_o with r/a for different materials and different maximum strains. This generality has a very important consequence, because it leads to a general criterion of applicability of the deformation theory of plasticity for any material in the strain-hardening range for this problem. The criterion now is that if the value of n for a given material is constant or approximately constant in the strain-hardening range, the deformation theory can be applied to the problem for this material. For the special case of infinitesimal strain, the condition that n is constant reduces to the condition that m is constant, which is the same condition obtained by Ilyushin (reference 16).

The maximum variation of α at any r/a is less than 10 percent for a variation of n from -0.15 to 0.4 (fig. 5(a)). Because for most materials m increases with γ, it can be seen from equation (14a) that m and γ_o affect n in an opposite manner, so that the variation of n with strain is small. The value of n for most materials and for any strain varies from -0.1 to 0.25 (references 17 to 19); only a small part of this variation is due to variation with strain for a given material. The variations of α during loading will then be expected to be very small for most materials; consequently, the deformation theory of plasticity is applicable within engineering accuracy to this problem.

It is also interesting to note the variations of γ/γ_o with r/a for different values of n. From figure 5(b) the curves of γ/γ_o against r/a near the hole, which is the region of interest, are close for values of n from -0.15 to 0.4.

The values of σ_r/τ, σ_θ/τ, ϵ_r/γ, and ϵ_θ/γ were calculated by equations (7a) and (8a) for the range of α considered (table II). The distributions of principal stresses and strains were obtained by the linearized solution for the following cases: $\gamma_o = 0.1871$, Inconel X; $\gamma_o = 0.3000$, Inconel X; and $\gamma_o = 0.4600$, 16-25-6. The results are plotted in figure 7 with results obtained in reference 2 for comparison. The examples $\gamma_o = 0.3000$, Inconel X, and $\gamma_o = 0.4600$, 16-25-6 are chosen because they show the greatest deviation in α and γ/γ_o between the linearized and the exact solutions. The example of $\gamma_o = 0.1871$, Inconel X is chosen because it has an average agreement between the two solutions. The value of n for this case is equal to 0.151; α and γ/γ_o at corresponding values of r/a can be obtained from table I by linear interpolation. The distributions of principal stresses and strains obtained by the linearized solution agree very well with those obtained by the exact solution even for the case of $\gamma_o = 0.4600$, 16-25-6, for which the agreement in γ/γ_o between the two solutions (fig. 6) is least.

Calculations were also made for the case of ideally plastic material (τ = constant) with the infinitesimal strain concept. The variations of α and γ/γ_o with r/a are the same as for the case of $n = 0$ (fig. 5). The distributions of principal strains were calculated for γ_o equal to 0.1871 and 0.4600 (fig. 8). The curves obtained by the exact solution for $\gamma_o = 0.1871$, Inconel X, and $\gamma_o = 0.4600$, 16-25-6 are also plotted in this figure. These two cases are chosen because the α and γ/γ_o curves deviate most from the curves of $n = 0$ (fig. 5). From the curves of α and γ/γ_o against r/a of $n = 0$ and the actual $\tau(\gamma)$ curve of Inconel X and 16-25-6, the distributions of principal stresses are calculated for the cases of $\gamma_o = 0.1871$ and $\gamma_o = 0.4600$, respectively; this procedure gives the approximate solution.

The principal stresses are also calculated for the ideally plastic materials. In this case τ = constant and is chosen equal to the value of τ_o for which the solutions are being compared. These distributions of principal stress along the radius, as well

as those obtained by linearized and exact solutions are plotted for comparison in figures 9(a) and 9(b) for $\gamma_o = 0.4600$, 16-25-6, and for $\gamma_o = 0.1871$, Inconel X, respectively. It can be seen from figure 8 that the principal strains obtained by the ideally plastic material with the infinitesimal strain concept (which is the same case as the approximate solution) gives good approximate results. As shown in figure 9, however, the principal stresses, especially the tangential stress (the most important part of the solution), obtained by the ideally plastic material are not good enough to approximate the actual results no matter which value of τ is used. With slight modification as described in the approximate solution (using α and γ/γ_o for $n = 0$ and the actual $\tau(\gamma)$ relation of the material), the principal stresses, especially the tangential stress, obtained agree much better with the exact solution. This simple approximate method can therefore give good results. It also indicates that the ratio of the strains along the radius to the maximum value and the ratio of principal stresses are essentially independent of the $\tau(\gamma)$ curve of the material and the maximum strain of the plate, but the stresses are very much dependent on the $\tau(\gamma)$ curve of the material. This result not only further confirms the conclusions obtained in reference 2, but also generalizes those results to most materials (that is, not limited by the $\tau(\gamma)$ curves of Inconel X and 16-25-6 previously investigated).

All the results and discussions are true only for this problem under plastic deformation in the strain-hardening range in which the elastic strains are small compared with the plastic strains, and neither time and temperature effects nor unloading are present.

CONCLUSIONS

The results obtained for a thin plate with circular hole in the strain-hardening range, in which the elastic strain is small compared with the plastic strain, show that:

1. The results obtained by the linearized solution agree very well with those obtained by the exact solution based on the deformation theory of plasticity. The amount of computation required is very much reduced by the linearization. With the tables or curves presented herein, the distributions of octahedral shear stress and strain as well as the principal stresses and strains can be obtained for a given material under a given maximum strain of the plate by a simple multiplication.

2. The variation of a parameter determined from the octahedral shear stress-strain curve of the material can be used as a simple general criterion of applicability of deformation theory for this problem.

3. The results previously obtained for Inconel X and 16-25-6 were extended to most materials: namely, the ratios of the strains along the radius to the maximum value and the ratio of principal stresses are essentially independent of the octahedral shear stress-strain curve of the material, but the stress distributions are very dependent on the material.

4. The results obtained for the ideally plastic material with the infinitesimal strain concept give good approximate values of principal strains, but not of principal stresses.

5. Sufficiently accurate values of principal stresses can be obtained by the approximate method of using the strains obtained by the ideally plastic material, together with the actual octahedral shear stress-strain relation of the material.

6. If a simple analytical function representing the octahedral shear stress-strain relation is required for analysis, the power-law approximation can be used.

Lewis Flight Propulsion Laboratory,
National Advisory Committee for Aeronautics,
Cleveland, Ohio, September 20, 1950.

REFERENCES

1. Nádai, A.: Plasticity. McGraw-Hill Book Co., Inc., 1931.

2. Wu, M. H. Lee: Analysis of Plane-Stress Problems with Axial Symmetry in Strain-Hardening Range. NACA TN 2217, 1950.

3. Nádai, A.: Plastic Behavior of Metals in the Strain-Hardening Range. Part I. Jour. Appl. Phys., vol. 8, no. 3, March 1937, pp. 205-213.

4. Davis, E. A.: Increase of Stress with Permanent Strain and Stress-Strain Relations in the Plastic State for Copper under Combined Stresses. Jour. Appl. Mech., vol. 10, no. 4, Dec. 1943, pp. A187-A196.

5. Davis, E. A.: Yielding and Fracture of Medium-Carbon Steel under Combined Stress. Jour. Appl. Mech., vol. 12, no. 1, March 1945, pp. A13-A24.

6. Osgood, W. R.: Combined-Stress Tests on 24S-T Aluminum-Alloy Tubes. Jour. Appl. Mech., vol. 14, no. 2, June 1947, pp. A147-A153.

7. Marin, Joseph, Faupel, J. H., Dutton, V. L., and Brossman, M. W.: Biaxial Plastic Stress-Strain Relations for 24S-T Aluminum Alloy. NACA TN 1536, 1948.

8. Marin, Joseph: Stress-Strain Relations in the Plastic Range for Biaxial Stresses. Jour. Franklin Inst., vol. 248, no. 3, Sept. 1949, pp. 231-249.

9. Fraenkel, S. J.: Experimental Studies of Biaxially Stressed Mild Steel in the Plastic Range. Jour. Appl. Mech., vol. 15, no. 3, Sept. 1948, pp. 193-200.

10. Davis, H. E., and Parker, E. R.: Behavior of Steel under Biaxial Stress as Determined by Tests on Tubes. Jour. Appl. Mech., vol. 15, no. 3, Sept. 1948, pp. 201-215.

11. Faupel, Joseph H., and Marin, Joseph: Tension-Compression Biaxial Plastic Stress-Strain Relations for Aluminum Alloys 24S-T and 2S-O. A.S.M. Preprint no. 35, presented at 32d Ann. Convention A.S.M. (Chicago), Oct. 23-27, 1950.

12. Davis, Evan A.: Plastic Behavior of Metals in the Strain-Hardening Range. Part II. Jour. Appl. Phys., vol. 8, no. 3, March 1937, pp. 213-217.

13. Nádai, A., and Donnell, L. H.: Stress Distribution in Rotating Disks of Ductile Material after the Yield Point Has Been Reached. APM-51-16, Trans. A.S.M.E., vol. 51, pt. 1, 1929, pp. 173-180; discussion, pp. 180-181.

14. Griffith, George E.: Experimental Investigation of the Effects of Plastic Flow in a Tension Panel with a Circular Hole. NACA TN 1705, 1948.

15. Stowell, Elbridge Z.: Stress and Strain Concentration at a Circular Hole in an Infinite Plate. NACA TN 2073, 1950.

16. Ilyushin, A. A.: The Theory for Small Elastic-Plastic Deformations. RMB-17, trans. by Grad. Div. Appl. Math., Brown Univ., for David W. Taylor Model Basin (Washington, D.C.), 1947. (Contract NObs-34166.)

17. MacGregor, C. W.: The Tension Test. Proc. A.S.T.M., vol. 40, 1940, pp. 508-534.

18. Low, John R., Jr., and Garofalo, Frank: Precision Determination of Stress-Strain Curves in the Plastic Range. Proc. Soc. Exp. Stress Anal., vol. IV, no. 2, 1947, pp. 16-24.

19. Hollomon, John H.: Tensile Deformation. Trans. A.I.M.E., Iron and Steel Div., vol. 162, 1945, pp. 268-289.

TABLE I - RELATIONS BETWEEN r/a AND γ/γ_o WITH α FOR DIFFERENT VALUES OF n

α	$n = -0.15$		$n = -0.1$		$n = 0$		$n = 0.1$		$n = 0.2$		$n = 0.3$		$n = 0.4$	
	r/a	γ/γ_o	r/a	γ/γ_o	r/a	γ/γ_o	r/a	γ/γ_o	r/a	γ/γ_o	r/a	γ/γ_o	r/a	γ/γ_o
0.5236	1.0000	1.0000	1.0000	1.0000	1.0000	1.0000	1.0000	1.0000	1.0000	1.0000	1.0000	1.0000	1.0000	1.0000
.6632	1.1866	.7895	1.1854	.7906	1.1831	.7929	1.1808	.7951	1.1786	.7972	1.1764	.7992	1.1743	.8012
.8378	1.5173	.5976	1.5089	.6019	1.4933	.6102	1.4789	.6180	1.4657	.6254	1.4534	.6324	1.4418	.6390
1.0123	2.0338	.4625	2.0043	.4706	1.9519	.4858	1.9066	.4997	1.8669	.5126	1.8318	.5246	1.8004	.5356
1.1519	2.7034	.3846	2.6329	.3958	2.5143	.4163	2.4174	.4347	2.3368	.4514	2.2682	.4668	2.2089	.4808
1.2741	3.6840	.3341	3.5346	.3478	3.2966	.3727	3.1143	.3946	2.9692	.4142	2.8508	.4319	2.7514	.4481
1.3788	5.2216	.3025	4.9200	.3184	4.4683	.3466	4.1442	.3709	3.8981	.3925	3.7040	.4119	3.5456	.4295
1.4486	7.2109	.2875	6.6852	.3046	5.9394	.3347	5.4309	.3605	5.0581	.3831	4.7707	.4033	4.5408	.4215
1.4835	8.9881	.2820	8.2515	.2997	7.2391	.3306	6.5679	.3569	6.0848	.3800	5.7173	.4004	5.4265	.4188
1.5010	10.3253	.2798	9.4272	.2978	8.2145	.3290	7.4231	.3555	6.8586	.3787	6.4321	.3993	6.0958	.4178
1.5184	12.2619	.2780	11.1295	.2963	9.6292	.3278	8.6651	.3544	7.9837	.3778	7.4730	.3985	7.0717	.4170
1.5359	15.4591	.2767	13.9420	.2951	11.9724	.3268	10.7274	.3537	9.8562	.3771	9.2083	.3978	8.7007	.4165

TABLE II - VALUES OF ϵ_r/γ, ϵ_θ/γ, σ_r/τ, AND σ_θ/τ FOR VARIOUS VALUES OF α

α	ϵ_r/γ	ϵ_θ/γ	σ_r/τ	σ_θ/τ
0.5236	-0.3536	0.7071	0	2.1214
.5934	- .3100	.7054	.1710	2.2016
.6632	- .2649	.7002	.3411	2.2713
.7505	- .2067	.6890	.5511	2.3424
.8378	- .1470	.6725	.7571	2.3961
.9250	- .0862	.6509	.9571	2.4312
1.0123	- .0247	.6243	1.1502	2.4481
1.0821	.0246	.5997	1.2980	2.4480
1.1519	.0739	.5721	1.4397	2.4361
1.2130	.1167	.5456	1.5582	2.4160
1.2741	.1590	.5172	1.6705	2.3868
1.3265	.1949	.4912	1.7622	2.3547
1.3788	.2302	.4639	1.8486	2.3160
1.4137	.2534	.4451	1.9036	2.2870
1.4486	.2763	.4255	1.9562	2.2547
1.4661	.2876	.4156	1.9818	2.2377
1.4835	.2988	.4056	2.0065	2.2201
1.4923	.3044	.4005	2.0186	2.2109
1.5010	.3100	.3954	2.0309	2.2017
1.5097	.3155	.3903	2.0426	2.1920
1.5184	.3210	.3851	2.0543	2.1825
1.5272	.3265	.3799	2.0659	2.1727
1.5359	.3320	.3747	2.0774	2.1629
1.5446	.3374	.3695	2.0887	2.1528
1.5533	.3428	.3642	2.0996	2.1424
1.5621	.3482	.3589	2.1107	2.1320
1.5708	.3536	.3536	2.1214	2.1214

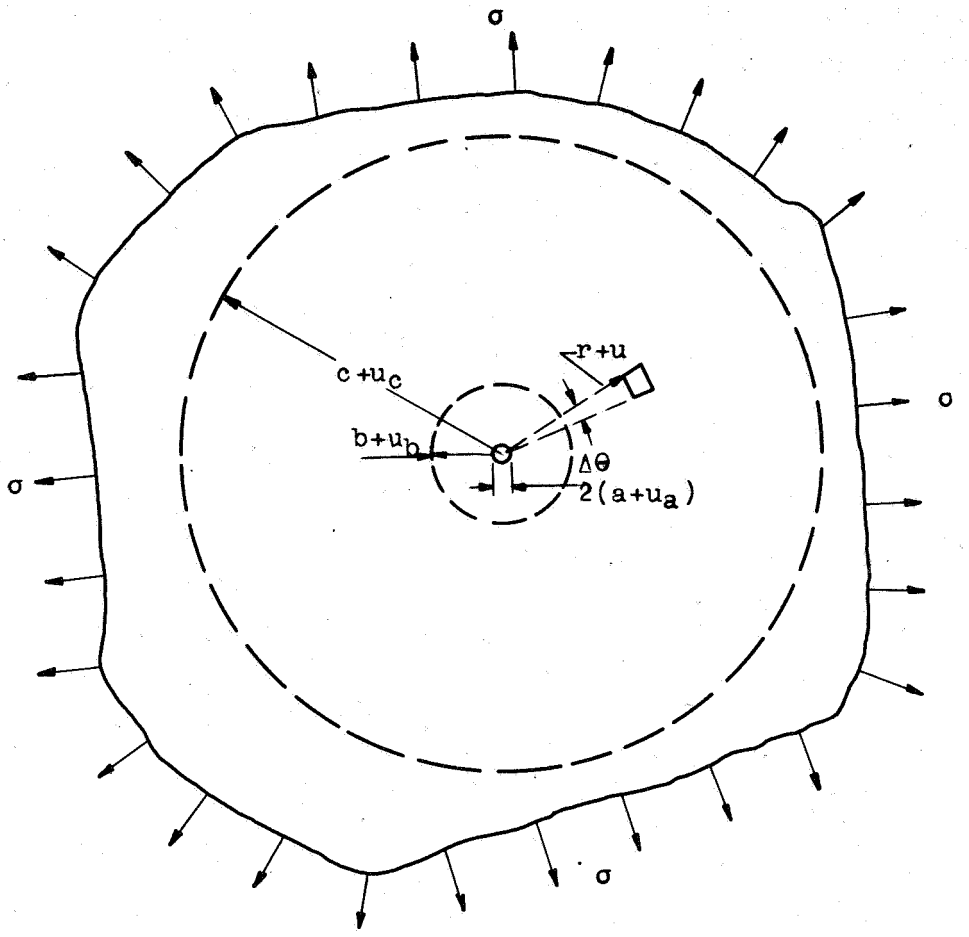

(a) Infinite plate with circular hole stressed uniformly in its plane in all directions.

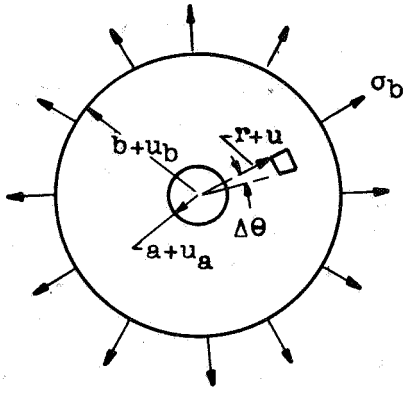

(b) Flat ring radially stressed.

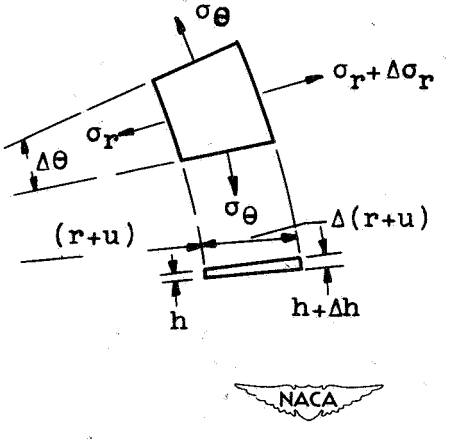

(c) Element of thin plate.

Figure 1. - Thin infinite plate with circular hole, flat ring, and its element in deformed state.

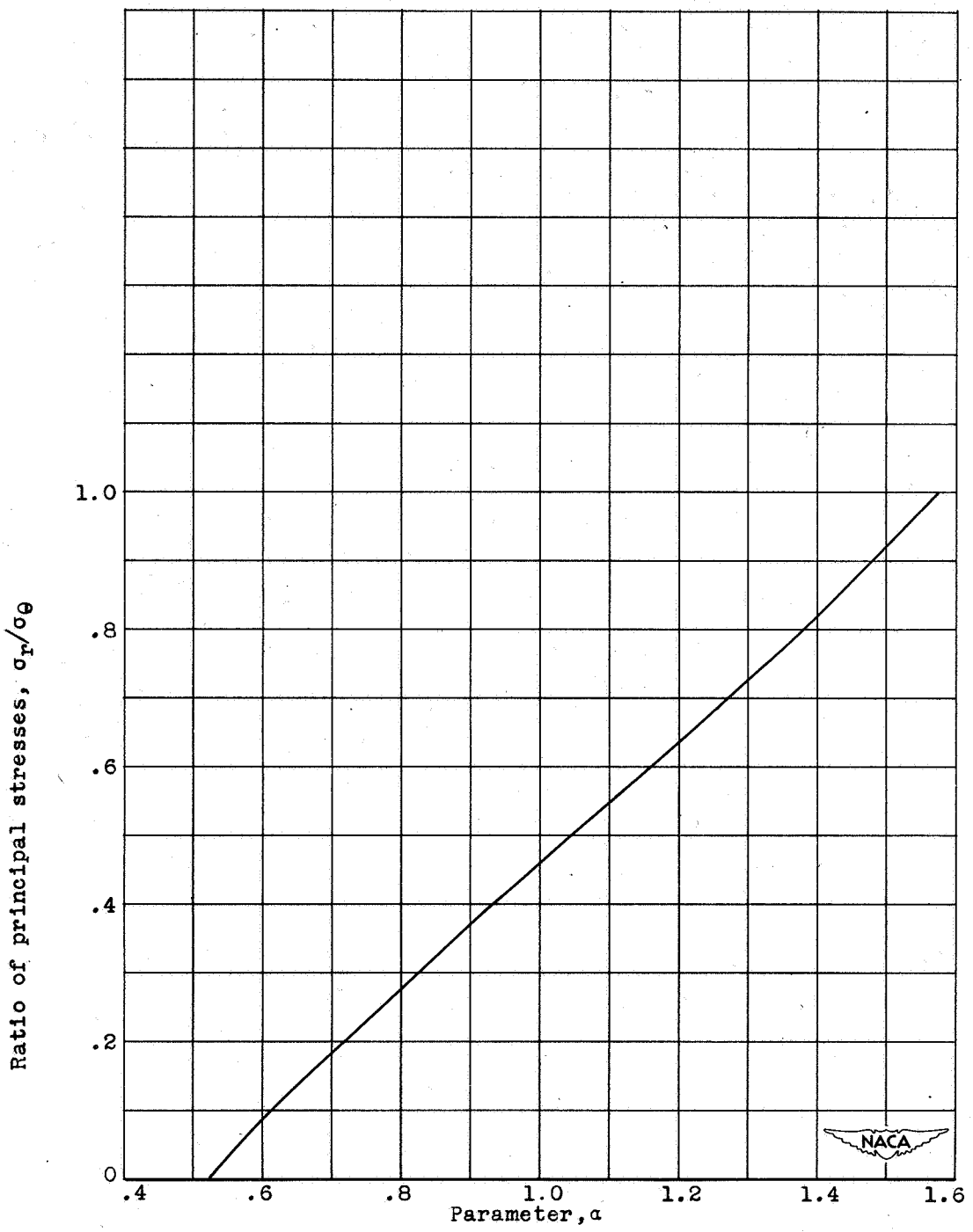

Figure 2. - Variation of ratio of principal stresses σ_r/σ_θ with parameter α.

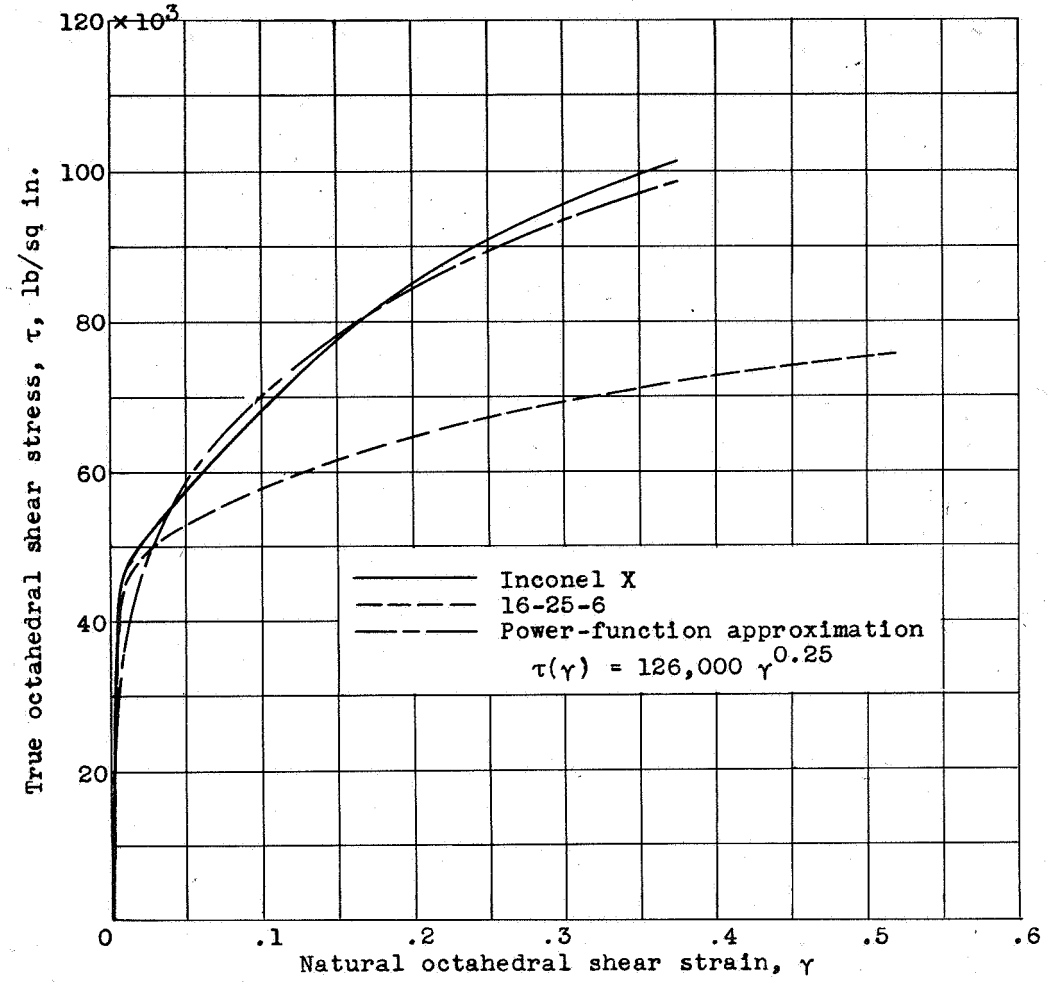

(a) Linear-scale plot.

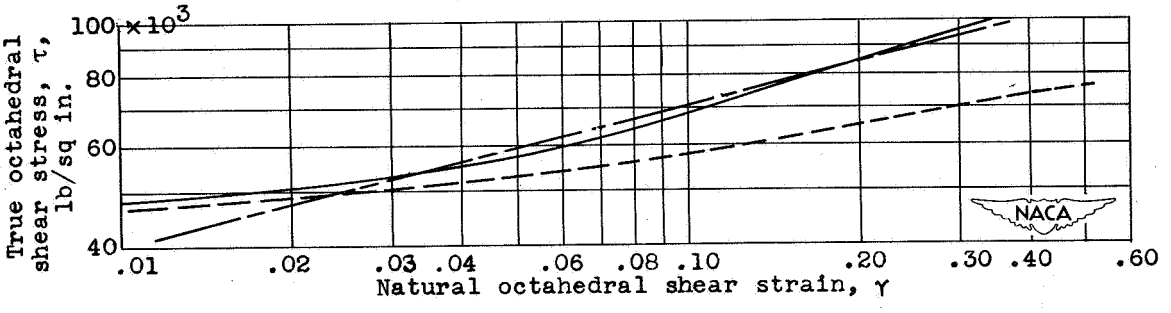

(b) Logarithmic-scale plot.

Figure 3. - Octahedral shear stress-strain curves.

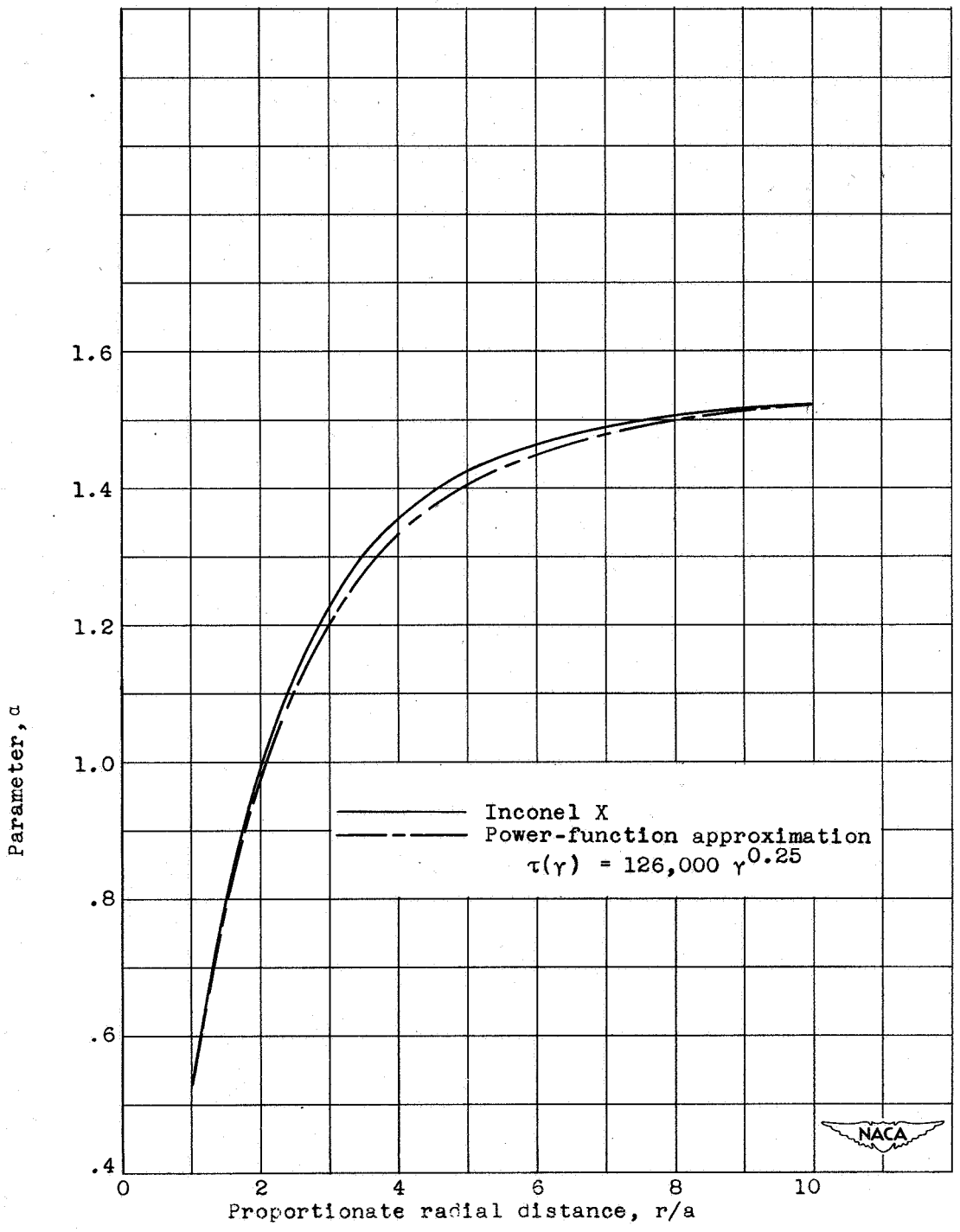

(a) Variation of parameter α with proportionate radial distance.

Figure 4. - Comparison of results obtained for $\tau(\gamma)$ curve of Inconel X and power-function approximation $\tau(\gamma) = 126{,}000\ \gamma^{0.25}$. $\gamma_o = 0.30$.

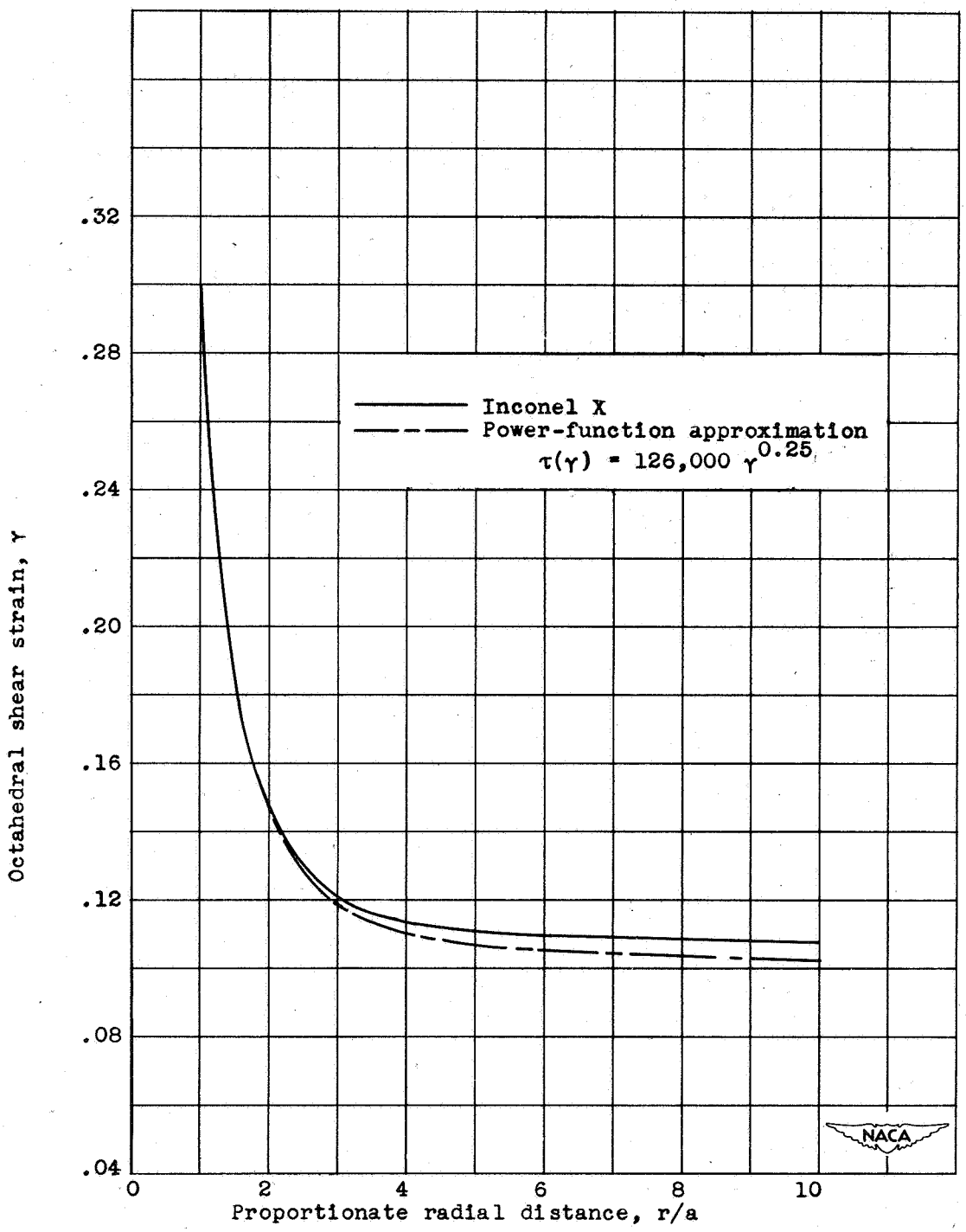

(b) Variation of octahedral shear strain with proportionate radial distance.

Figure 4. - Continued. Comparison of results obtained for $\tau(\gamma)$ curve of Inconel X and power-function approximation $\tau(\gamma) = 126{,}000\ \gamma^{0.25}$. $\gamma_o = 0.30$.

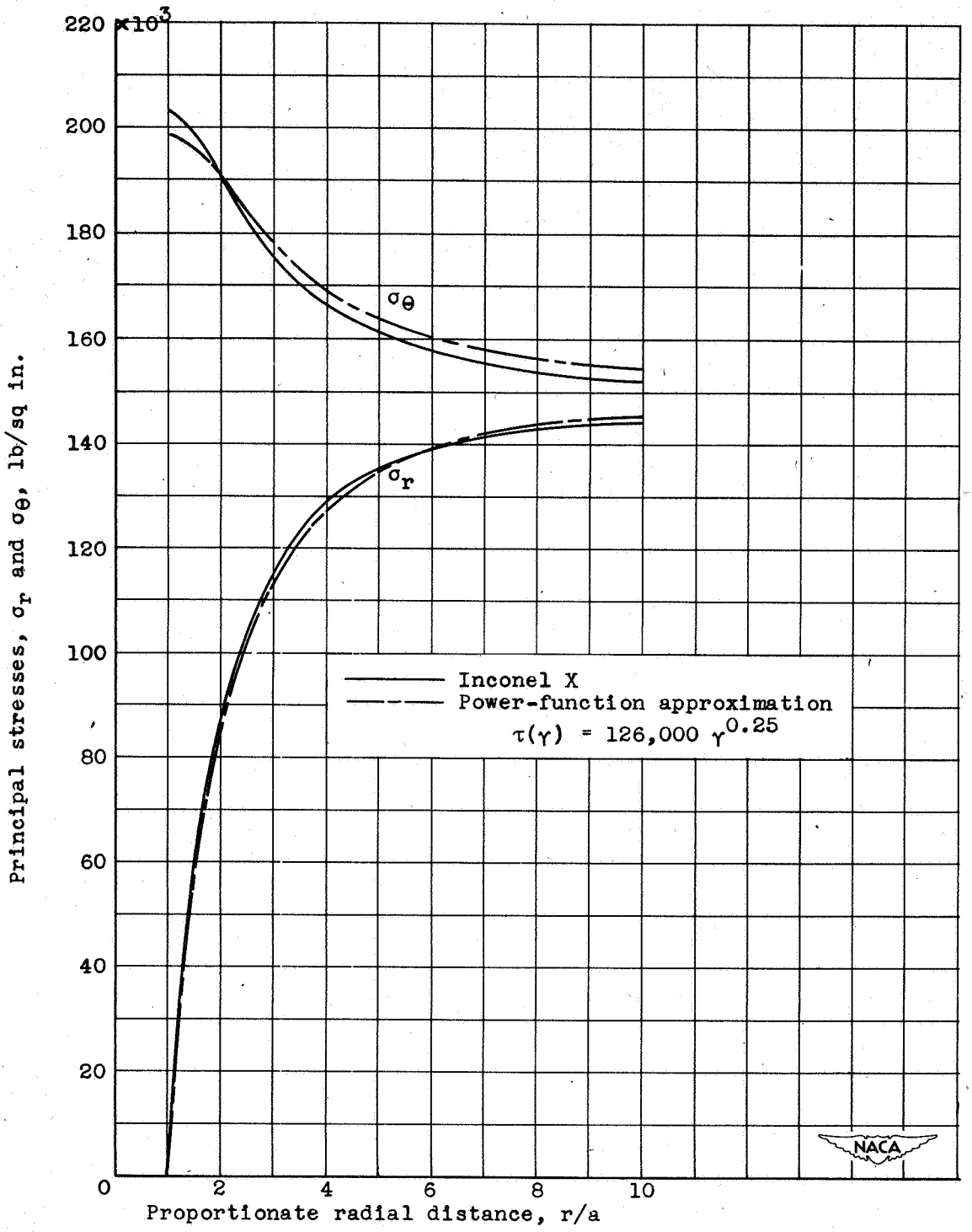

(c) Variation of principal stresses with proportionate radial distance.

Figure 4. - Continued. Comparison of results obtained for $\tau(\gamma)$ curve of Inconel X and power-function approximation $\tau(\gamma) = 126{,}000\ \gamma^{0.25}$. $\gamma_o = 0.30$.

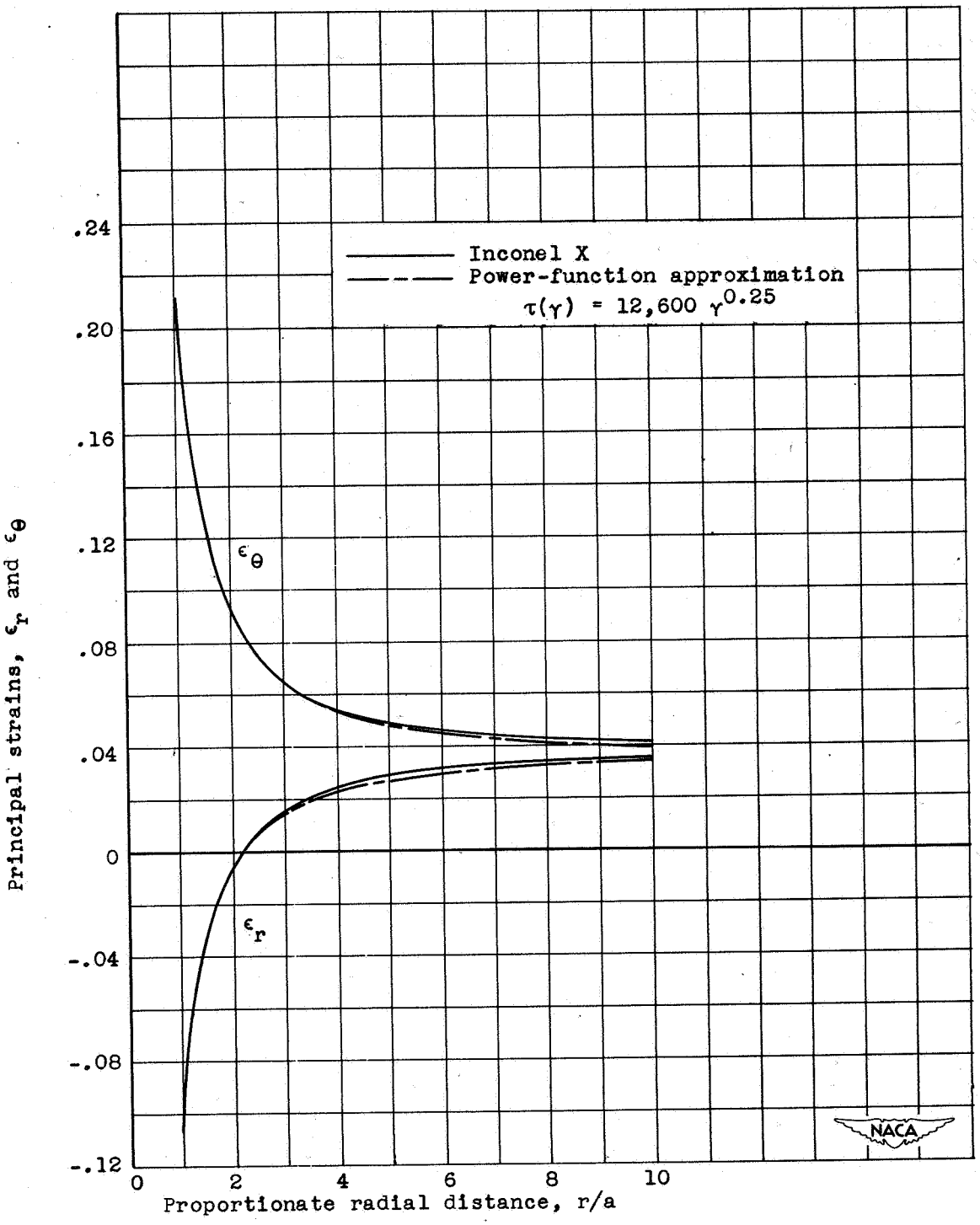

(d) Variation of principal strains with proportionate radial distance.

Figure 4. - Concluded. Comparison of results obtained for $\tau(\gamma)$ curve of Inconel X and power-function approximation $\tau(\gamma) = 126{,}000\ \gamma^{0.25}$, $\gamma_o = 0.30$.

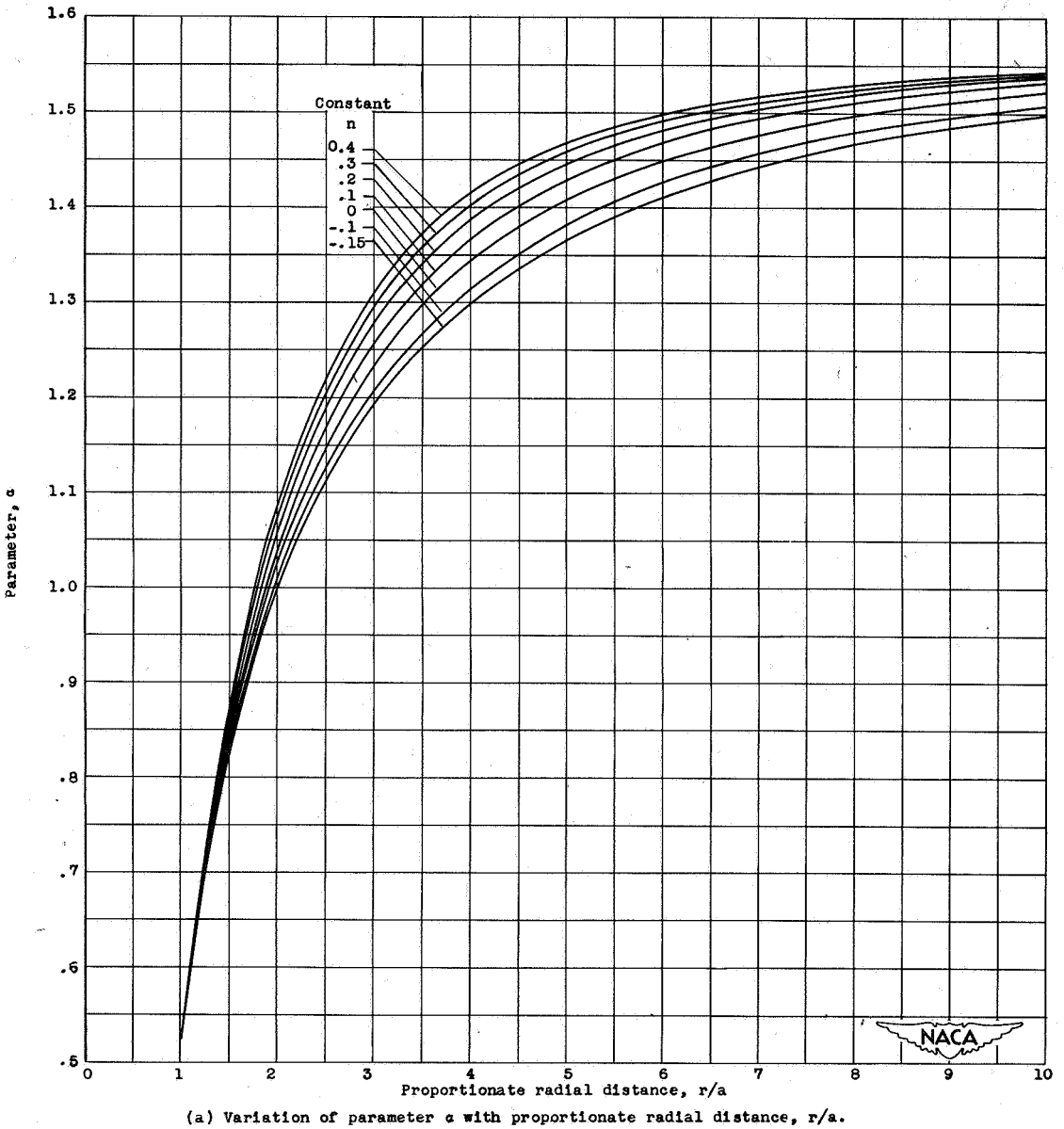

(a) Variation of parameter α with proportionate radial distance, r/a.

Figure 5. - Variation of parameter α and the ratio of octahedral shear strain to octahedral shear strain at hole γ/γ_o with proportionate radial distance r/a obtained by linearized solution for various values of n.

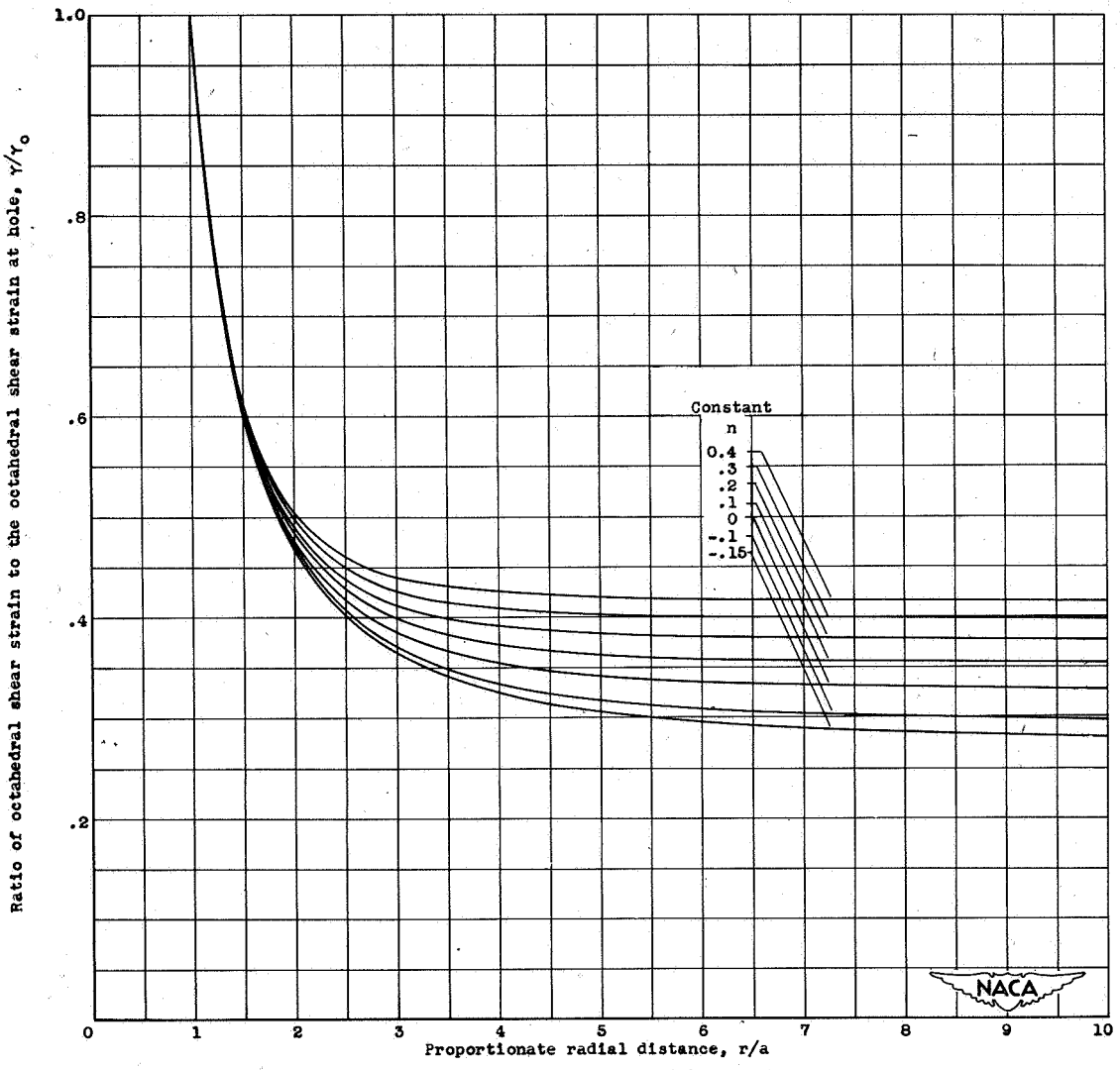

(b) Variation of ratio of octahedral shear strain to octahedral shear strain at hole γ/γ_o with proportionate radial distance r/a.

Figure 5. - Concluded. Variation of parameter α and the ratio of octahedral shear strain to octahedral shear strain at hole γ/γ_o with proportionate radial distance r/a obtained by linearized solution for various values of n.

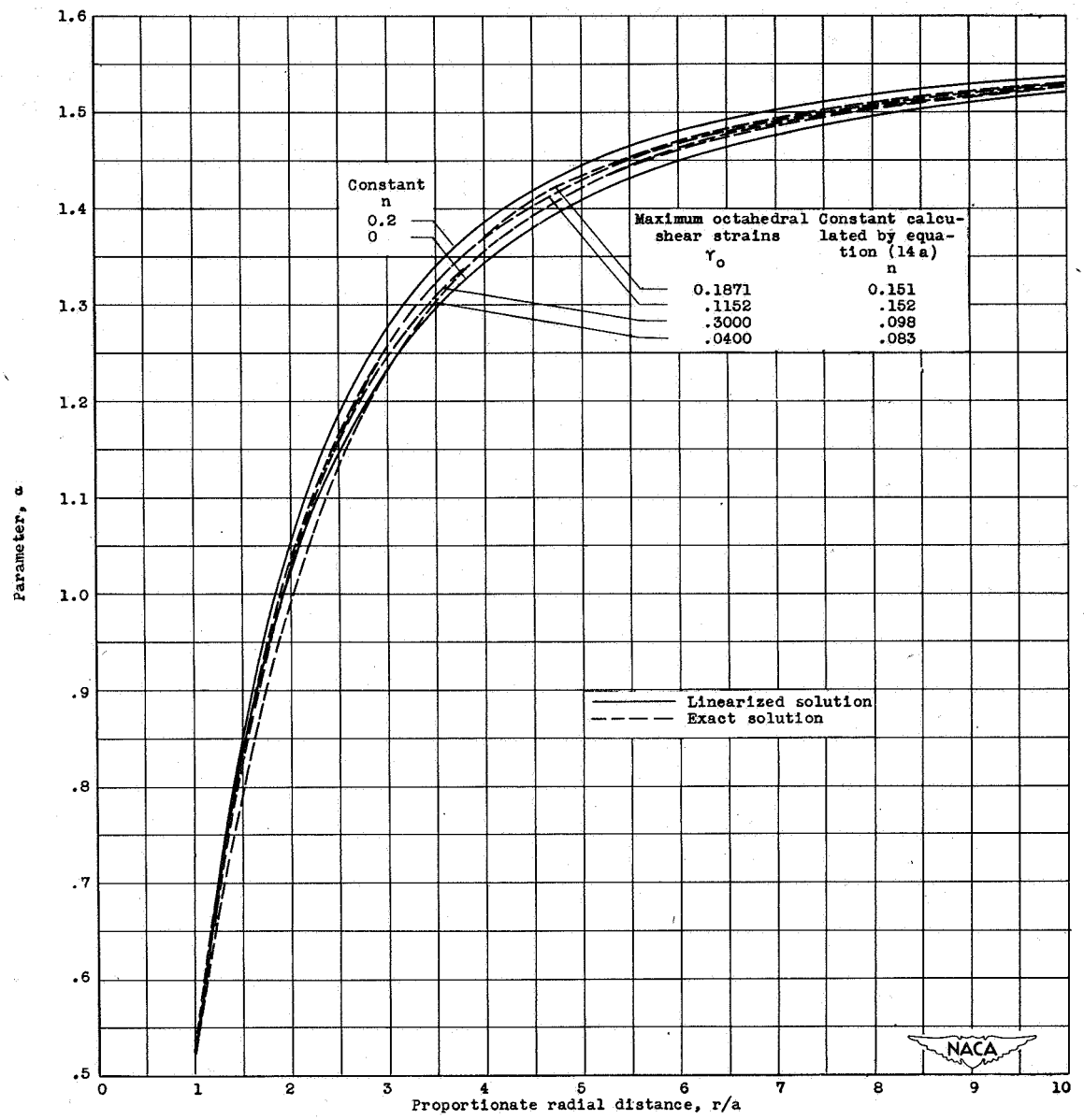

(a) Variation of parameter α with proportionate radial distance; Inconel X.

Figure 6. - Comparison of variation of parameter α and ratio of octahedral shear strain to octahedral shear strain at hole γ/γ_o with proportionate radial distance r/a obtained by linearized solution and by exact solution.

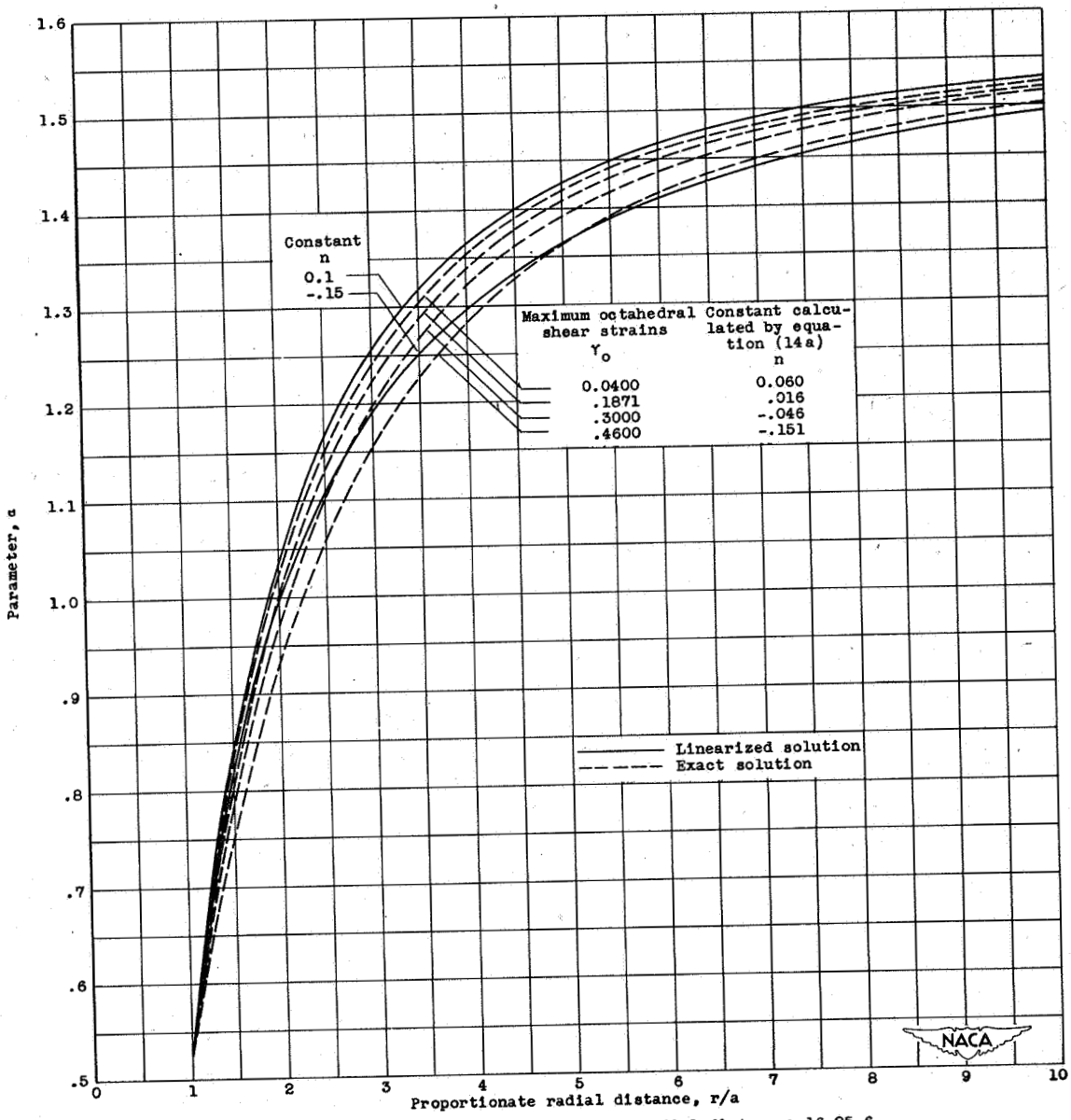

(b) Variation of parameter α with proportionate radial distance; 16-25-6.

Figure 6. - Continued. Comparison of variation of parameter α and ratio of octahedral shear strain to octahedral shear strain at hole γ/γ_o with proportionate radial distance r/a obtained by linearized solution and by exact solution.

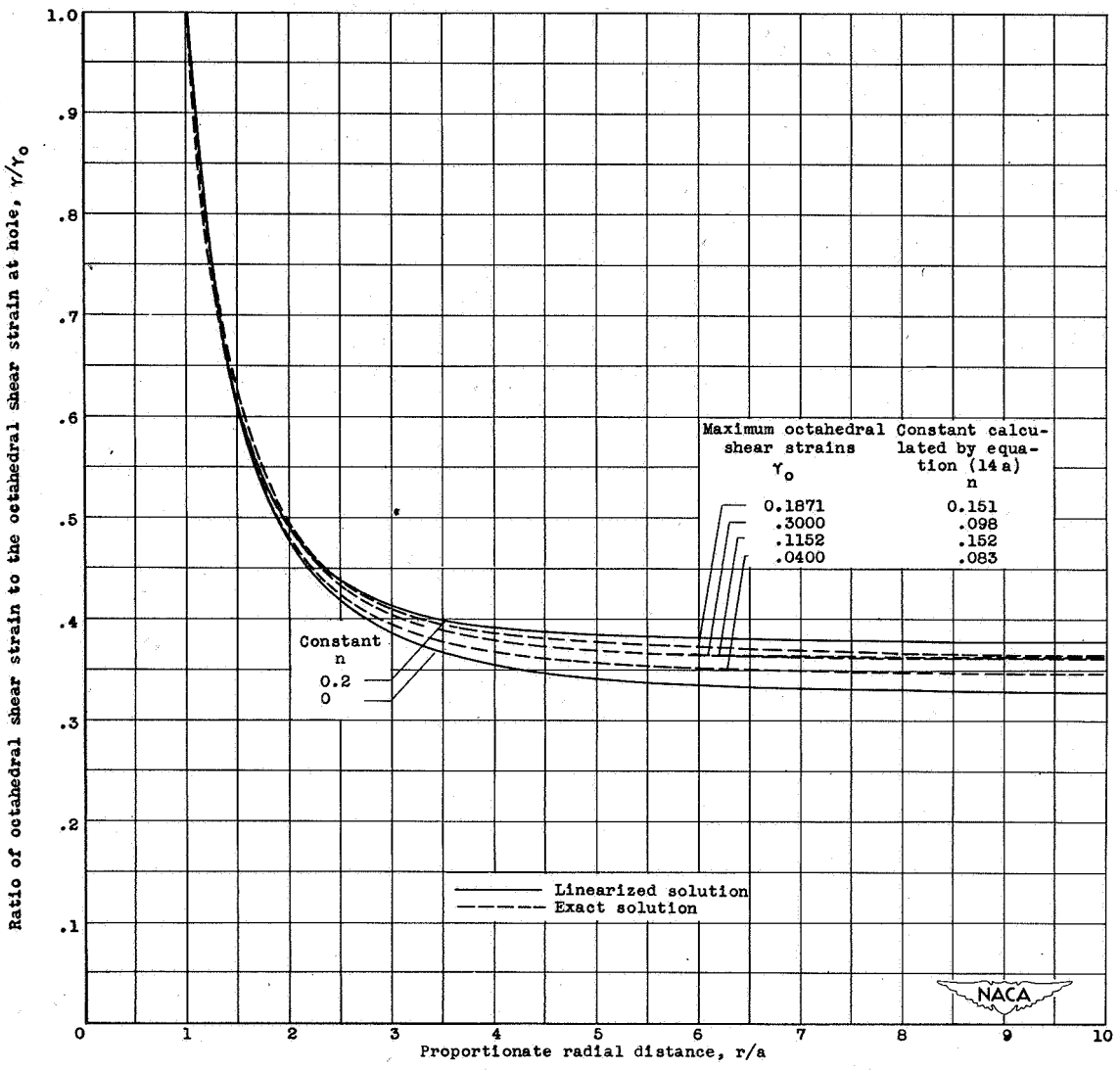

(c) Variation of ratio of octahedral shear strain to maximum octahedral shear strain at hole γ/γ_o with proportionate radial distance; Inconel X.

Figure 6. - Continued. Comparison of variation of parameter α and ratio of octahedral shear strain to octahedral shear strain at hole γ/γ_o with proportionate radial distance r/a obtained by linearized solution and by exact solution.

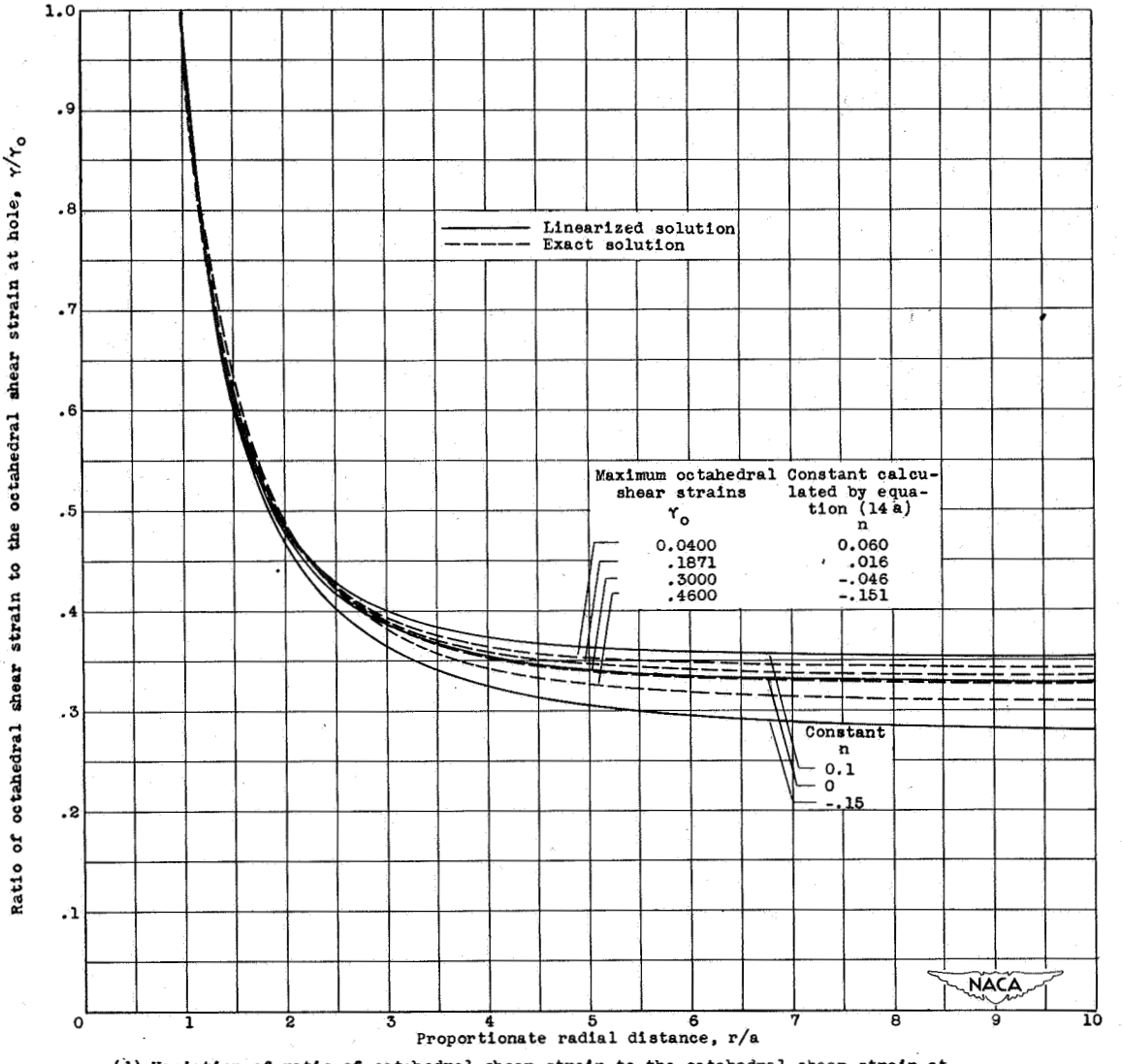

(d) Variation of ratio of octahedral shear strain to the octahedral shear strain at hole γ/γ_o with proportionate radial distance; 16-25-6.

Figure 6. - Concluded. Comparison of variation of parameter α and ratio of octahedral shear strain to octahedral shear strain at hole γ/γ_o with proportionate radial distance r/a obtained by linearized solution and by exact solution.

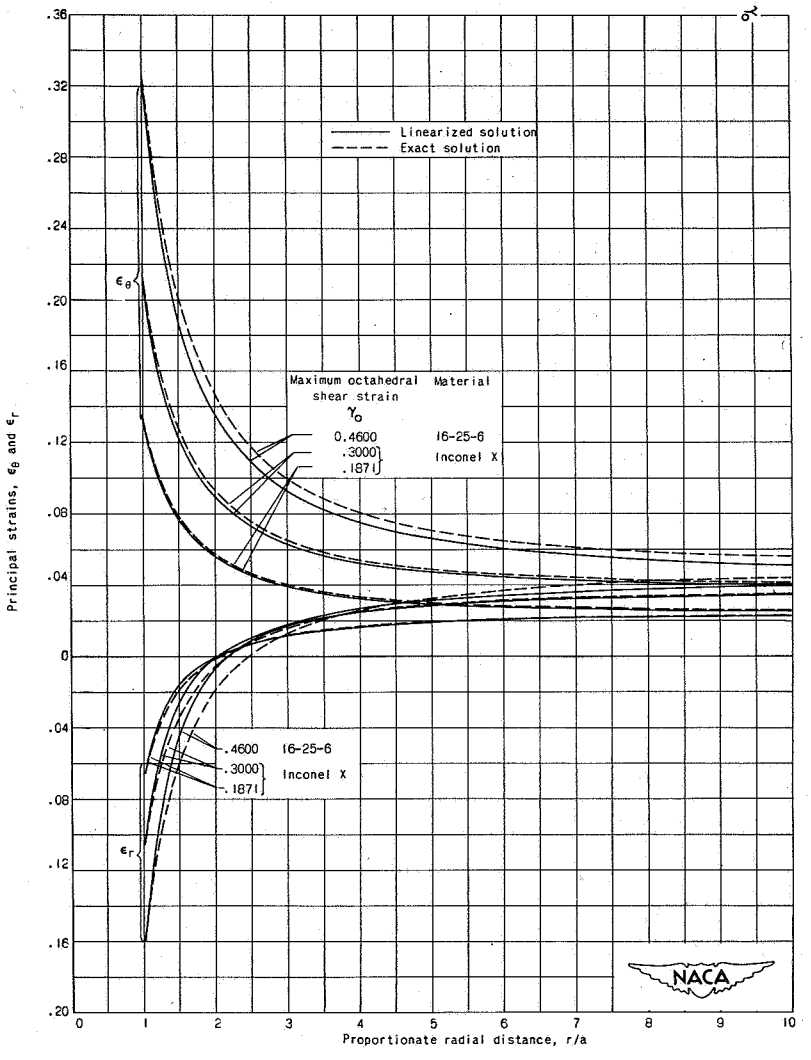

(a) Variation of principal strains with proportionate radial distance.

Figure 7. - Comparison of principal stresses and strains obtained by linearized solution and exact solution.

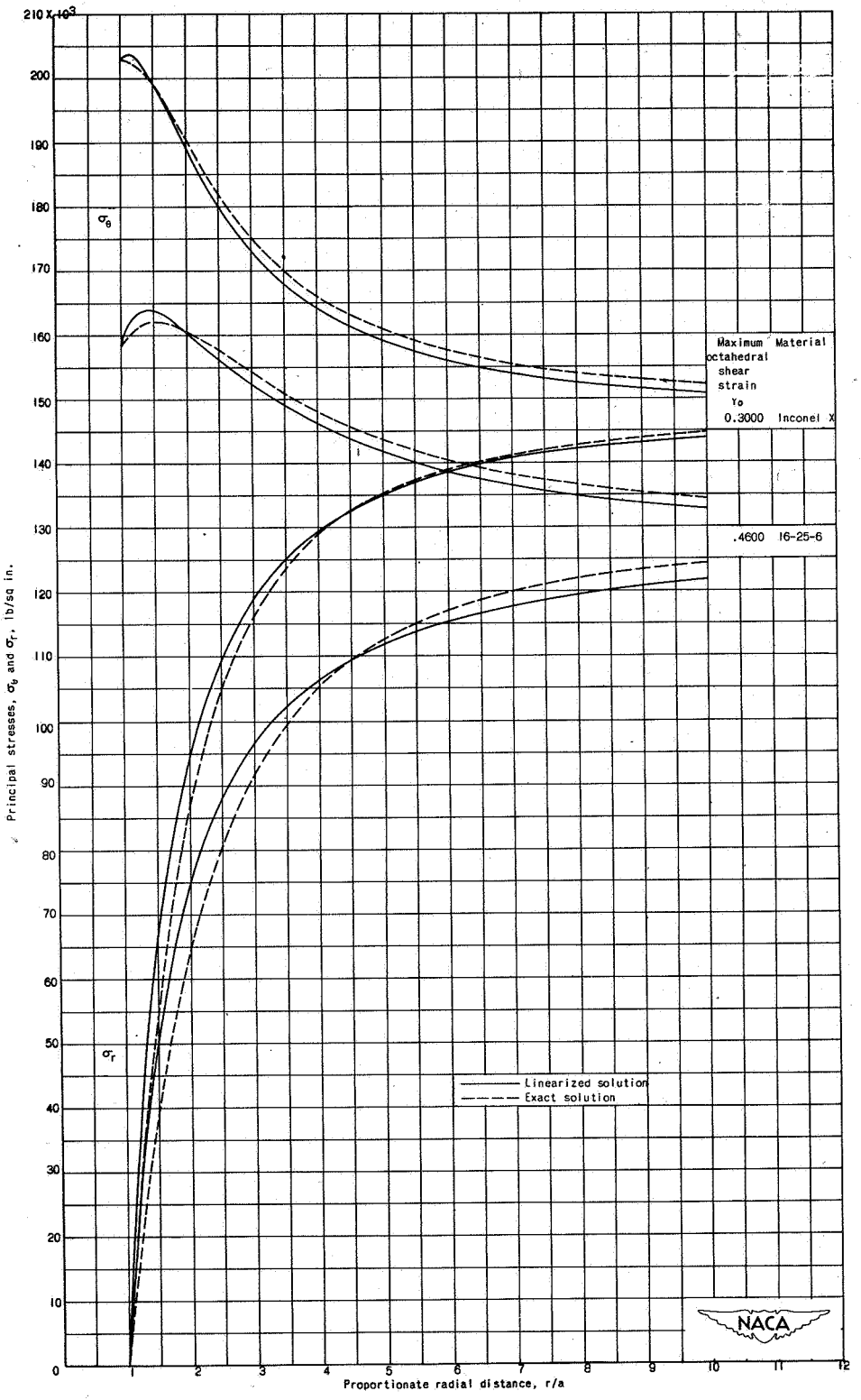

(b) Variation of principal stresses with proportionate radial distance.

Figure 7. - Concluded. Comparison of principal stresses and strains obtained by linearized solution and exact solution.

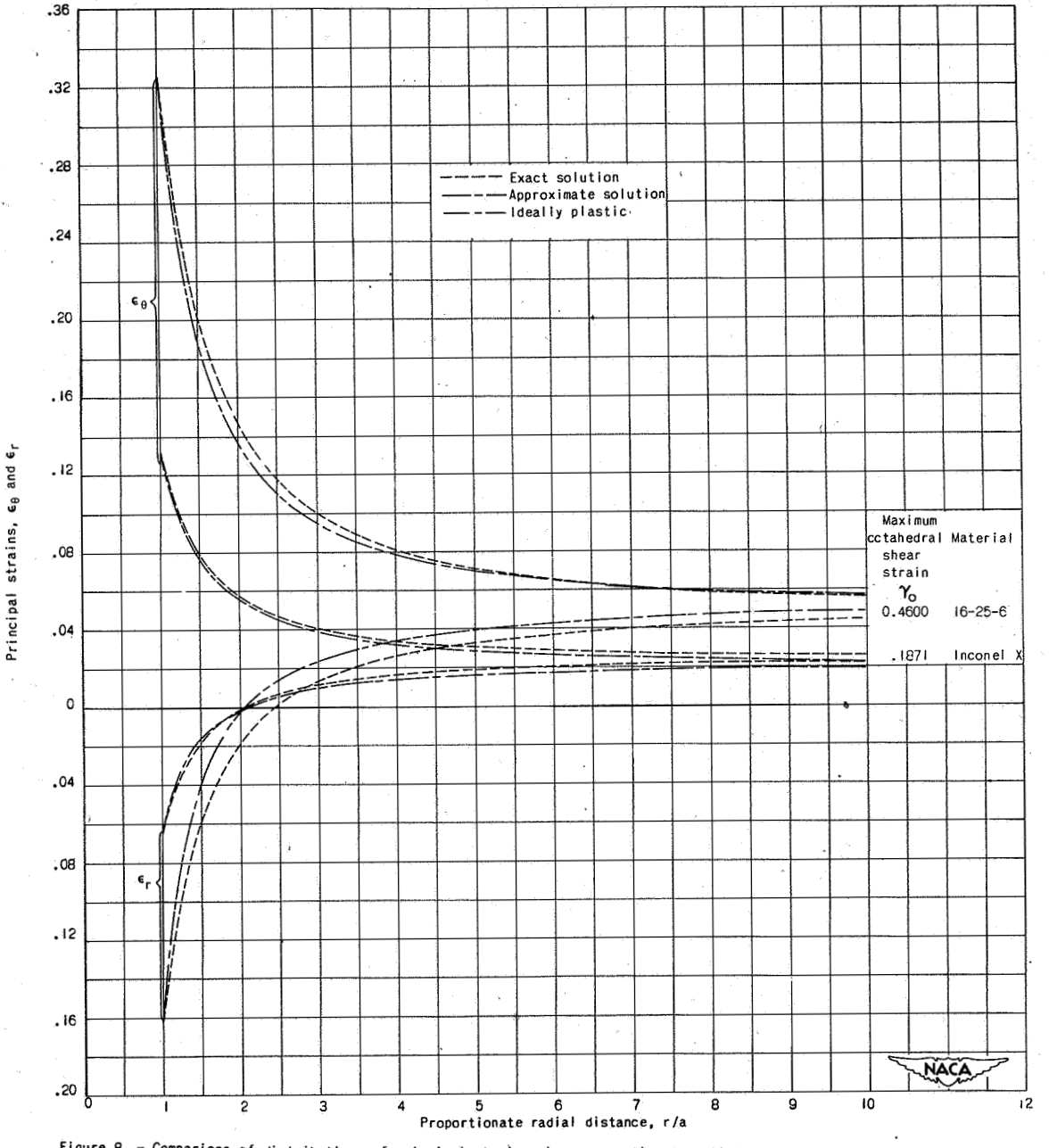

Figure 8. - Comparison of distributions of principal strains along proportionate radial distance obtained by approximate solution and ideally plastic with exact solution.

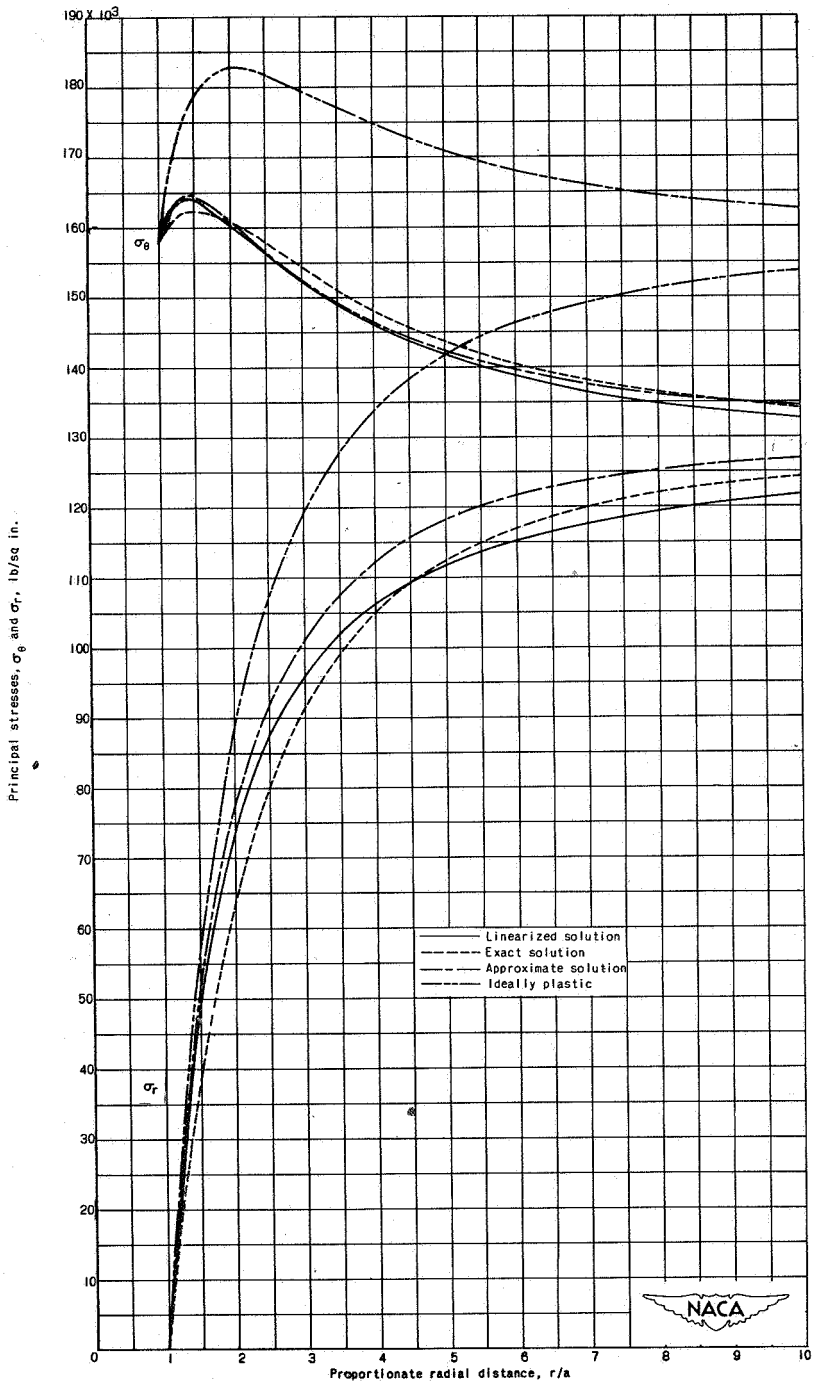

(a) γ_0 = 0.46, 16-25-6.

Figure 9. - Comparison of distributions of principal stresses along proportionate radial distance obtained by different methods.

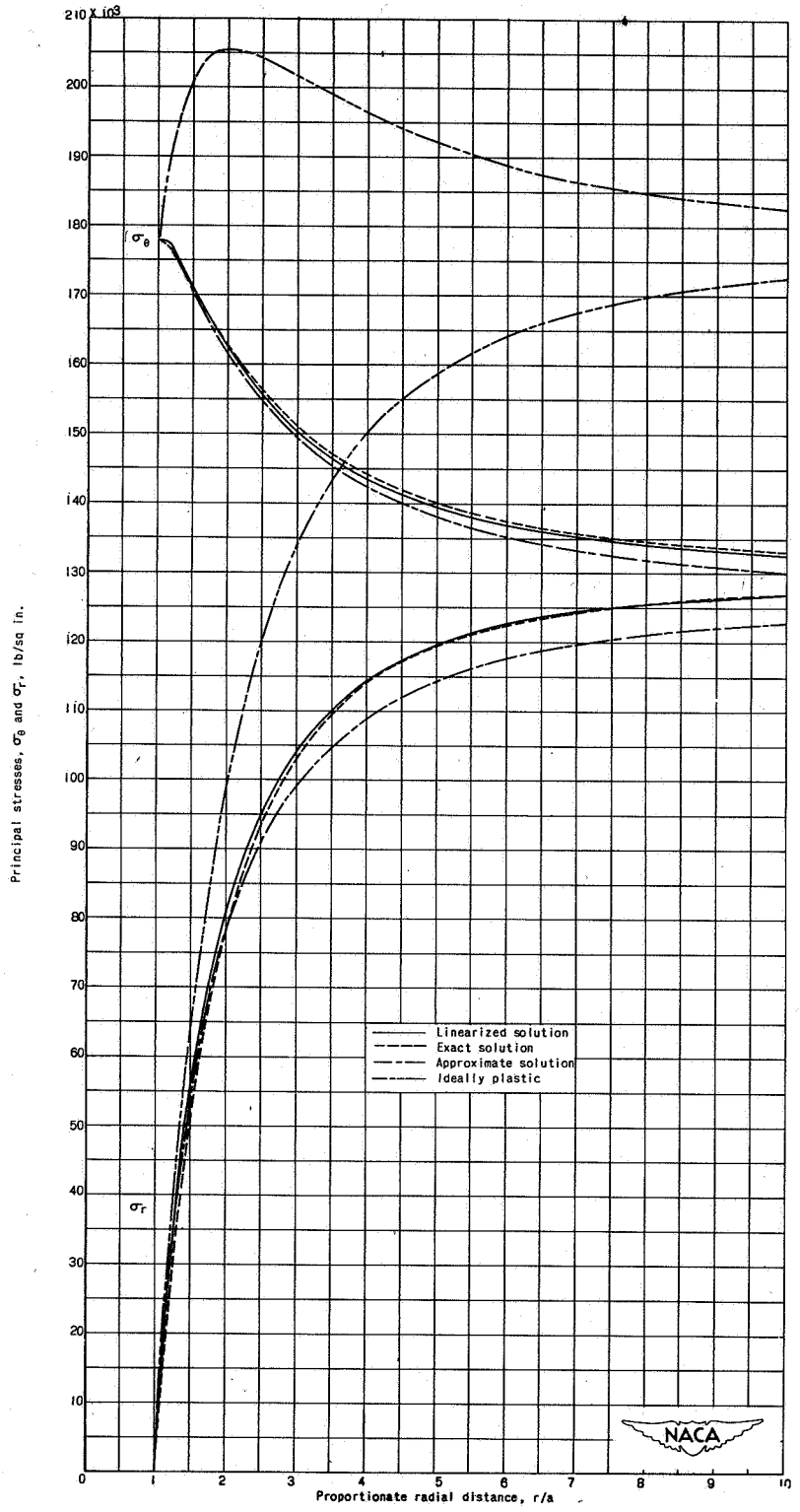

(b) $\gamma_0 = 0.1871$, Inconel X.

Figure 9. - Concluded. Comparison of distributions of principal stresses along proportionate radial distance obtained by different methods.